BRIGHAM YOUNG UNIVERSITY

GEOLOGY STUDIES

VOLUME 36 • 1990

BRIGHAM YOUNG UNIVERSITY GEOLOGY STUDIES

Volume 36, 1990

CONTENTS

A Publication of the
Department of Geology
Brigham Young University
Provo, Utah 84602

Brigham Young University Geology Studies is published by the Department of Geology. This publication consists of graduate student and faculty research within the department as well as papers submitted by outside contributors. Each article submitted by BYU faculty and outside contributors is externally reviewed by at least two qualified persons.

ISSN 0068-1016
5-90 600 44626

Stratigraphy and Sedimentology of the Middle Jurassic Carmel Formation in the Gunlock Area, Washington County, Utah

DRU R. NIELSON
DCM/Joyal Engineering, Walnut Creek, California 94595

Thesis Chairman: J. KEITH RIGBY

ABSTRACT

The Carmel Formation near Gunlock is composed of 240 m of shallow-marine to peritidal sedimentary rocks that accumulated in two major transgressions and one regression, composed of seven, second-order, shallowing-upward cycles in an arid climate near the southern margin of the Middle Jurassic Western Interior seaway. The sedimentology of the Co-op Creek Member and approximately 100 m of previously unreported section including the Crystal Creek and parts of the Paria River(?) Members is described from 10 laterally equivalent measured sections spanning nearly 15 km.

Sedimentary features include bivalve-inhabited bored hardgrounds, oyster colonies, salt-hopper casts, mudcracks, raindrop impressions, fenestrae, algal stromatolites, tidal channels, evaporite solution breccia, ripple marks, cross-bedding, and seven volcanic ash beds that give isotopic and fission track ages from Late Callovian to Early Oxfordian. Gastropods, bivalves, *Pentacrinus* columnals, bryozoans, ostracodes, radiolarians(?), foraminifers, echinoids, corals, and trace fossils of the *Trypanites*, *Skolithos*, and *Cruziana* ichnofacies occur. Diagenetic influences include evaporite dissolution, replacement crystallization, neomorphism, oxidation, and minor dolomitization. Geochemical analyses of carbonate lithologies document inverse relationships between insoluble residue percentages and that of Ca/Mg ratios.

INTRODUCTION

The Carmel Formation near Gunlock, northwest of St. George, Utah, records a variety of sedimentary environments near what was the southern end of the Middle Jurassic Western Interior seaway (Blakey and others 1983). These rocks are the westernmost exposures of marine Jurassic rocks in the Cordilleran region. Over five square kilometers of excellent exposures of Carmel Formation exist near Gunlock. These rocks contain fine examples of shallow marine to tidal flat carbonates and document two periods of major transgression and regression with second- and third-order transgressive and regressive cycles and lateral shifts of environments. The Carmel in the Gunlock area is here divided into six informal members labeled A–F. Members A–D are part of the Co-op Creek Member of Doelling (1988). Members E and F are believed to be equivalent, respectively, to the Crystal Creek and lower Paria River(?) Members of Thompson and Stokes (1970).

This report describes the sedimentary facies, structures, and spatial relationships within these local members. From these descriptions a model of deposition is postulated. This report also discusses the effects of diagenesis on the rocks, the rock's fossil character, and geochemical analyses of the major constituents within the carbonate lithologies. The stratigraphic location of seven volcanic ashes within the Carmel in the study area is recorded as well as preliminary fission track and isotopic ages obtained from some of these horizons.

LOCATION

The study area is in southwestern Utah (fig. 1) near the Beaver Dam Mountains on the western margin of the transition zone between the High Plateaus and Basin and Range Provinces. Access is by paved and unpaved roads from St. George and Gunlock. Approximate locations of the measured sections are shown on figure 1. Detailed locations are given on the heading of each section descrip-

An excerpt of a thesis submitted to the Department of Geology, Brigham Young University, in partial fulfillment of the requirements for the degree of Master of Science, October 1988.

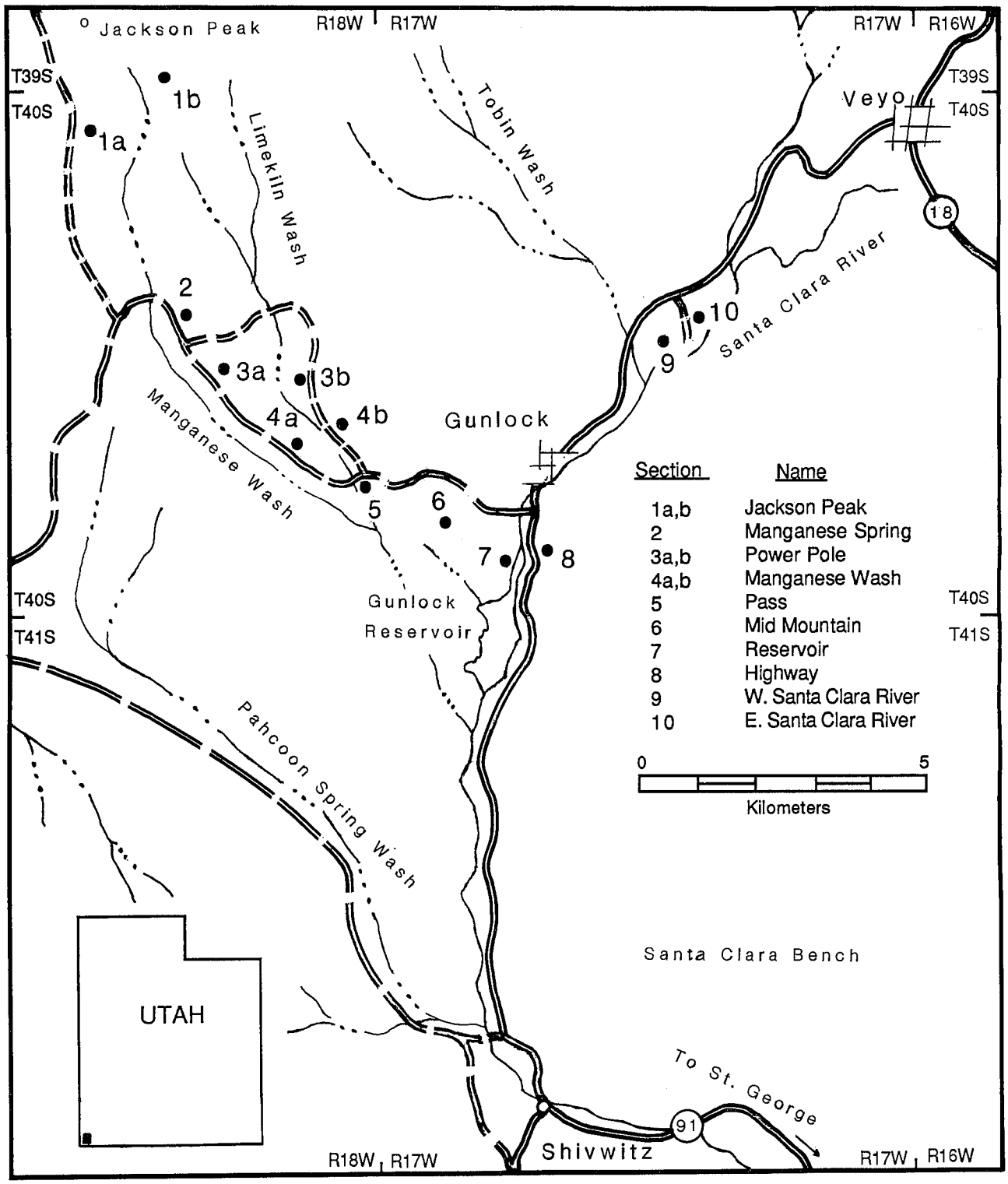

FIGURE 1.—*Index map of the study area in the Beaver Dam Mountains area showing locations of measured sections.*

tion in the appendix of Nielson (1988). Section descriptions are also available from the Department of Geology at Brigham Young University.

METHODS

Ten sections were measured along linear outcrop trends near Gunlock, Utah, during the 1987 and 1988 field seasons (fig. 1). The sections were measured to the nearest 0.1 m with a 1.5 m Jacob's staff. Individual units were correlated between sections by walking bedding planes where feasible or through aerial photographic methods and/or by the relationships to key stratigraphic marker beds such as volcanic ashes. The color of each unit was described using the GSA rock-color chart (Goddard and others 1984). Grain sizes were classified according to the Wentworth-Udden grain-size scale (Lewis 1986, p. 59).

Seventy thin sections were made from representative samples of each carbonate rock type as well as from consolidated terrigenous-dominated lithologies. Thin sections were stained with Alizarine Red S solution to distinguish calcite from dolomite, as described by Friedman (1959). Binocular and petrographic microscopes were used to identify the microfauna, sedimentary structures, textures, and constituent mineral grains. Unconsolidated terrigenous sediments were examined under a binocular microscope.

Seventy-one carbonate units from sections 1 and 10 were analyzed for calcium and magnesium using an Inductively Coupled Plasma Atomic Emission Spectroscope (ICPAES). One gram of each sample was dissolved in concentrated hydrochloric acid. The undissolved portion was filtered, dried, and weighed. The filtered solution was diluted with distilled water. Parts per million (ppm) calcium and magnesium were determined using a 1 to 1000 dilution. Standards for each analyzed element were prepared with stockroom chemicals by Dr. Angus U. Blackham from the Department of Chemistry at Brigham Young University.

Carbonate nomenclature in this study follows the scheme of Embry and Klovan (1971) as modified from Dunham (1962), which classifies rocks on the basis of depositional texture. The use of prefixes like "lime" in "lime mudstone" is used to distinguish Dunham's carbonate mud from the more commonly associated terrigenous "mudstone," used here in the sense of Ingram (1953) as a fine-grained, nonfissile sedimentary rock consisting of at least 50% silt and clay with no connotation concerning the relative percentages of silt and clay. Modifiers such as "sandy-oolitic" in "sandy-oolitic grainstone" were added to convey additional description of minor constituents. Terrigenous rocks described in this study were classified according to a similar modifying scheme as proposed by Friedman and Sanders (1978, p. 189).

PREVIOUS WORK

Localized studies of the Carmel Formation, similar to this one, have been done in various parts of Utah. Bordine (1965), Bullock (1965), and Hinman (1957) analyzed the facies and paleoecology of the Carmel-equivalent Twin Creek Limestone in north central Utah. Bagshaw (1977) and Dover (1969) studied the lithology and paleoecology of the lower Carmel rocks in the San Rafael Swell, and Fritz (1977) and Lowrey (1976) did the same for rocks in the Uinta Mountains. Richard's (1958) study concerned the cyclicity of the Carmel in northeastern Utah. Taylor (1981) explored the facies, paleoenvironments, and depositional history of the Carmel Formation at its type locality near Carmel Junction in southwestern Utah.

Regional studies and reviews that include the Carmel–Twin Creek Formation within Utah include those by Blakey and others (1983), Caputo (1980), Cashion (1967), Freeman (1976), Geesaman (1979), Imlay (1953, 1967, 1980), Peterson and Pipiringos (1979), Thompson and Stokes (1970), Voorhees (1978), Williams (1952), and Wright and Dickey (1963a, 1963b, 1978a, 1978b, 1979).

No detailed study of the Carmel Formation has been done in the Gunlock area. However, section 7 was measured as part of regional studies of the Carmel and associated units by Wright and Dickey (1979). Peterson and Pipiringos (1979) and Voorhees (1978) also measured stratigraphic sections near section 7 of this study. In other regional studies, Baker, Dane, and Reeside (1936), E. F. Cook (1957), and Reeside and Bassler (1922) included measured stratigraphic sections of Carmel rocks exposed 16 km east of the study area in Diamond Valley. Short stratigraphic descriptions of the Carmel Formation within the study area were included in reports associated with geologic mapping of the Gunlock area by E. F. Cook (1957, 1960), Hintze (1986), Hintze, Embree, and Anderson (in press), McCarthy (1959), and Wiley (1963).

In conjunction with this study, students of Brigham Young University's geology field camp measured preliminary stratigraphic sections of the lower parts of the formation in the Gunlock area (Rigby 1986a, 1986b).

STRATIGRAPHIC NOMENCLATURE

The Carmel Formation is one of the most conspicuous marine sequences in the dominantly nonmarine Mesozoic section (fig. 2) of the Colorado Plateau (Hintze 1988). It was first reported by John Wesley Powell (1875) as a distinct unit in the Flaming Gorge Group above the Vermillion Cliffs during his exploration of the Colorado

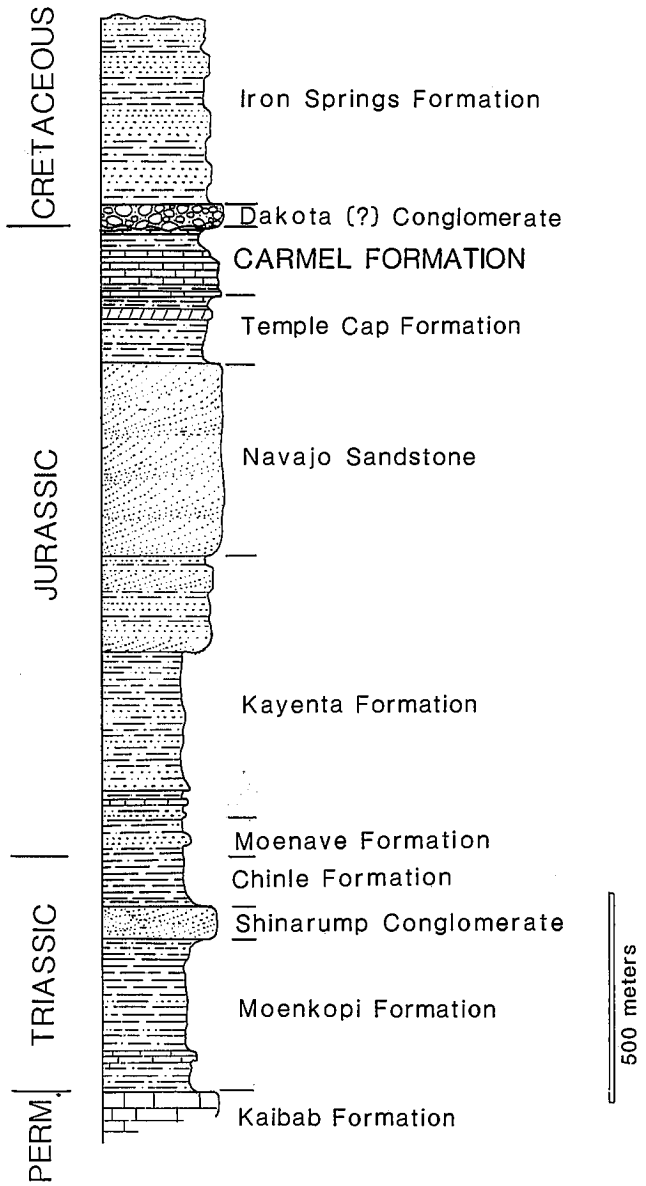

FIGURE 2.—*Generalized columnar section of Mesozoic rocks exposed in the Beaver Dam Mountains showing the position of the Carmel Formation.*

River and its tributaries. These rocks were later named the Carmel Formation in 1926 at a meeting of H. E. Gregory, R. C. Moore, and J. B. Reeside (Wilmarth 1938, p. 351). Exposures near Mount Carmel Junction, observed by Gregory and Noble (1923), were designated as the type locality, but they were not described until 1931 by Gregory and Moore. Previous workers like Leith and Harder (1908) and Walcott (Cross and Howe 1905, Gregory and Noble 1923) called Carmel strata such names as "Marine Jurassic" and "Carboniferous Homestake Limestone." Later, Mackin (1954) showed that Leith and Harder's "Carboniferous Homestake Limestone" of Iron County was equivalent to the well-known Jurassic Carmel Formation to the east. The earliest report using the formal name Carmel Formation was by Gilluly and Reeside (1928).

Even following its formal proposal, Carmel and related strata have been subject to frequent misidentification. Gross lithologic similarity of units within the Carmel to other Jurassic formations caused pioneering stratigraphers in southwestern Utah to miscorrelate Carmel units with the Entrada, Curtis, Summerville, and Morrison Formations (fig. 3). Later stratigraphic problems related to the Carmel Formation were primarily concerned with member nomenclature.

Formal members of the Carmel Formation in southwestern and south central Utah were proposed by Cashion (1967) and Thompson and Stokes (1970) as the Kolob Limestone, Crystal Creek, Paria River, Winsor, and Wiggler Wash Members from bottom to top. Thompson and Stokes (1970) correlated some of the lower Carmel members westward from the type locality of the formation near Mount Carmel Junction to one measured by E. F. Cook (1957) a few kilometers northeast of the Beaver Dam Mountains. The lower members have been generally accepted by subsequent workers in southwestern Utah. The name Kolob, however, was previously used for a latite flow unit near Cedar City, Utah (Averitt 1962; Keroher 1970, p. 402). As a result, workers in southwestern Utah have referred to the lower limestone unit of the Carmel as either the "limestone member" of Cashion (1967) or followed Wright and Dickey (1963b) and called it the Judd Hollow Member. The extension of the name Judd Hollow Tongue also has lithologic difficulty because the Judd Hollow was originally defined in south central Utah as a horizontally bedded sandstone unit equivalent to the lower part of the Carmel at the type section (Keroher 1970, p. 377; Phoenix 1963). H. H. Doelling and F. D. Davis (1989) have simplified the nomenclatural problem by redefining the limestone member of Cashion (1967) as the Co-op Creek Member of the Carmel.

PALEOGEOGRAPHY

Climate, location, and tectonic setting of the western margin of the craton in North America resulted, during the Jurassic, in the development of widespread ergs, sabkhas, and shallow restricted seas. The Jurassic western coast of North America was characterized by an "Andean-type" magmatic arc with sea-floor subduction occurring during emplacement of Middle Jurassic batholithic intrusions and related volcanics (Dickinson 1981). In early Middle Jurassic time, a shallow epeiric sea advanced southward across western Utah and into southeastern Nevada (Peterson 1988a) in a retroarc to craton-margin

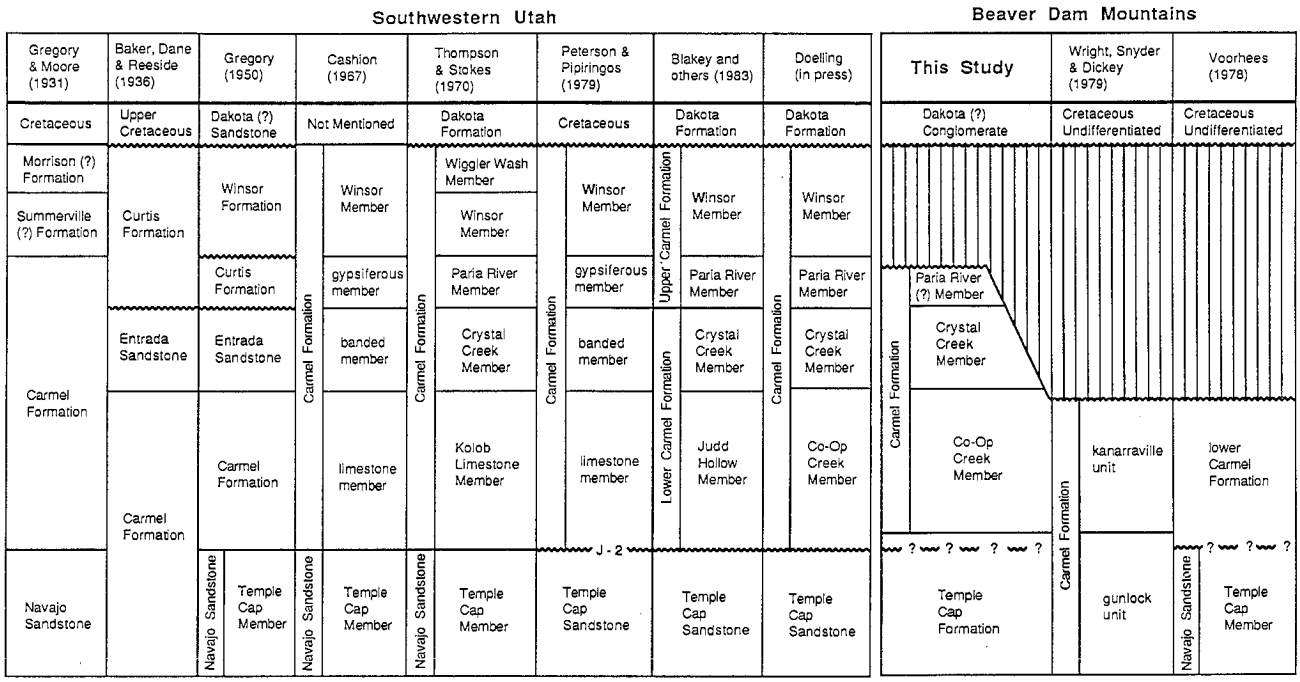

FIGURE 3.—*Stratigraphic nomenclature of the Carmel Formation and associated strata as applied by various workers in southwestern Utah and the Beaver Dam Mountains.*

basin possibly resulting from interplate convergence occurring at this time along the western margin of North America.

During this period the Gunlock area lay near the southern margin of the long, narrow, occasionally restricted seaway (fig. 4). The eastern depositional edge of this seaway is well documented (Blakey and others 1983), but the original western depositional limit is not preserved. Marine deposits probably did not extend more than a few tens of kilometers west of their present eroded edges since no Jurassic sediments have been found in Utah west of the Sevier geanticline, and thicknesses of sections on the east side of that structure show rapid westward thinning east of where they pass beneath Sevier-age thrust faults (Hintze 1988). During Carmel deposition the region was about 20° north paleolatitude within the trade wind belt (Kocurek and Dott 1983) and had a hot, arid climate marked by periodic storms. Frakes (1979) postulated that the global mean temperature was 10° C warmer in the Mesozoic than at present.

The siliciclastic rocks that occur in Middle Jurassic units of the Western Interior (Arapien Shale, Carmel and Twin Creek Formations) were probably derived from the remnant highlands of the ancestral Rockies to the east and the Mogollon highlands to the south of the Carmel–Twin Creek seaway. The lack of coarse terrigenous sediments suggests that Middle Jurassic subsidence probably reflected tectonic events that took place farther west than the Sevier Orogenic belt (Heller and others 1986) and that the orogenic activities in the Western Cordillera had not progressed to the point that associated tectonic elements were highly elevated. Magmatic activity associated with a Jurassic magmatic arc, west and southwest of the study area in a belt across Nevada, California, and Arizona (Allmendinger and Jordan 1981; Armstrong and Suppe 1973; Dickinson 1977; Stanley, Jordan, and Dott 1979), must have been far enough away from the Carmel–Twin Creek seaway to only allow accumulations of volcanic ash in low-energy sedimentary environments of this time. Chapman (1986, 1987) documented the existence of large rhyolitic boulders and cobbles in the uppermost part of the Carmel in south central Utah and has plotted the existence of dated Jurassic source granites for these boulders in the southwestern U.S. She suggested that the closest dated granites that may be related to the rhyolitic materials are ones noted by Armstrong and Suppe (1973) at 160–189 Ma in the Ivanpah Mountains of California, 300 km from the Gunlock area.

STRATIGRAPHY

TEMPLE CAP FORMATION

The Temple Cap is a nonresistant series of reddish brown, gypsiferous, dolomitic mudstone and sandstone beds that overlies the Navajo Sandstone and underlies the Carmel Limestone. A massive bed of gypsum, up to 5 m

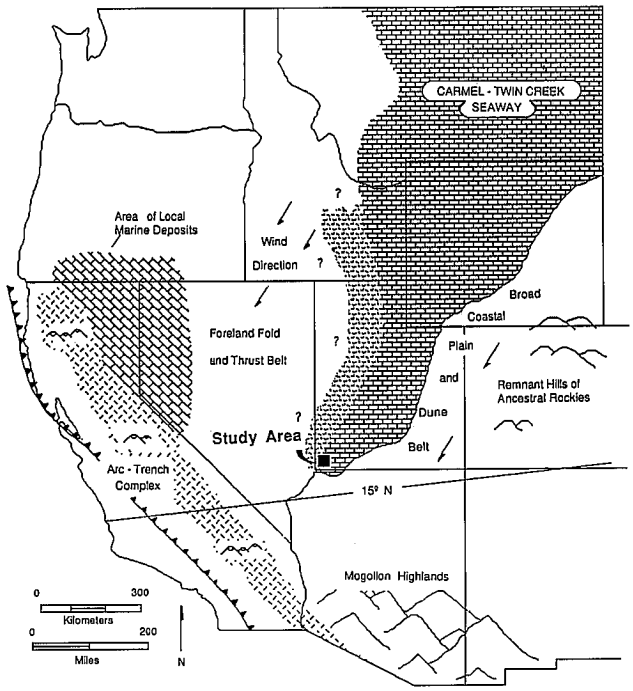

FIGURE 4.—*Middle to Late Jurassic paleogeography of the western United States showing extent of the Carmel–Twin Creek seaway. Incomplete limestone pattern bordered by question marks indicates unknown western depositional limit of the Carmel–Twin Creek seaway (modified from Blakey and others 1983, Imlay 1956, Kocurek and Dott 1983, and Peterson 1988a).*

thick, occurs in the upper part of the Temple Cap a few meters below the basal limestone of the Carmel Formation. This gypsum is an excellent marker bed that accumulated as a shoreward forerunner of the Carmel Limestone in the Gunlock region. This gypsum and interbedded red-bed sequence was deposited on a sabkha to tidal flat, where the shoreline transgressed and regressed across a nearly flat surface in the Gunlock area. The Temple Cap Formation consists of an upward-increasing gypsiferous red-bed sequence that culminates in the major transgressive gypsum bed, which is followed by a minor regression and accumulation of interbedded yellow gray and red siltstone. This regression was followed abruptly by the lower Carmel transgression, which produced the basal Carmel limestone. The Temple Cap Formation is about 450 m thick.

CARMEL FORMATION

The Carmel in southern Utah was designated as Middle Jurassic in age by Imlay (1980) based on certain bivalves in Carmel strata that are known elsewhere in the Western Interior region only in beds that contain Middle Jurassic ammonites. A Middle Jurassic age is also supported by the presence of the coral *Astrocoenia*, which has been found only in Bajocian age beds of Montana and Wyoming, and by the discovery of the bryozoan *Mesenteripora*, which is usually restricted to the Bathonian of northern Europe (Taylor 1981). A Middle Jurassic isotopic age of 165 Ma has been reported by Marvin and others (1965) from a volcanic ash in the Gunlock area that appears to correlate to this study's ash A in upper member B. A 165 Ma age has also been reported by Hintze (1986) from ash E in the lower part of member E. Brent Everett and Bart Kowallis, from the Department of Geology at Brigham Young University, are currently working on fission track and argon-argon dating of all seven volcanic ashes identified in the Carmel near Gunlock during this study. Their preliminary results indicate that the ashes range from late Callovian to early Oxfordian age (personal communication). An Oxfordian age conflicts with Callovian ages of strata younger than the Carmel (Entrada, Curtis, and Summerville Formations) according to Imlay (1980), and resolution of this discrepancy awaits further research.

Carmel rocks of the Gunlock area have been mentioned only briefly in prior regional correlations. This most likely resulted from their isolation from other outcrops of Carmel rocks and the mistaken assumption that sections measured near Gunlock Reservoir, in which only the lower limestone of the Carmel is preserved below a regional unconformity, is representative of all exposures of the formation in the area. However, measured sections 1, 3, and 4, of the present study contain not only the Co-op Creek Limestone Member, but also parts of the Crystal Creek and Paria River(?) Members.

Carmel rocks are exposed in the study area at Gunlock Reservoir, in isolated exposures along the Gunlock-Veyo highway east of the reservoir, and in exposures in cuestas and strike valleys that extend from the west shore of the reservoir westward to the vicinity of Square Top Mountain and Jackson Peak (fig. 5). The lower, calcareous part of the formation (member C) forms the shoulders of the prominent cuesta above a strike valley carved in the underlying reddish brown Temple Cap Formation. The upper, silty part of the formation (member D) forms the upper half of the cuesta and the strike valley and slope below the next cuesta capped by cliff-forming Dakota(?) Conglomerate.

Other Carmel exposures are present northeast of Gunlock along the Santa Clara River (fig. 6). Here exposures are part of a volcanic-covered belt of Jurassic rocks that extend eastward from the Santa Clara River valley around the southern margin of the Pine Valley Mountains. The belt of Jurassic rocks is broken at the west and is offset to the south along the Gunlock Fault. This fault is displayed along the Gunlock-Veyo highway near the top of section 9. There the fault juxtaposes olive gray limestone of the

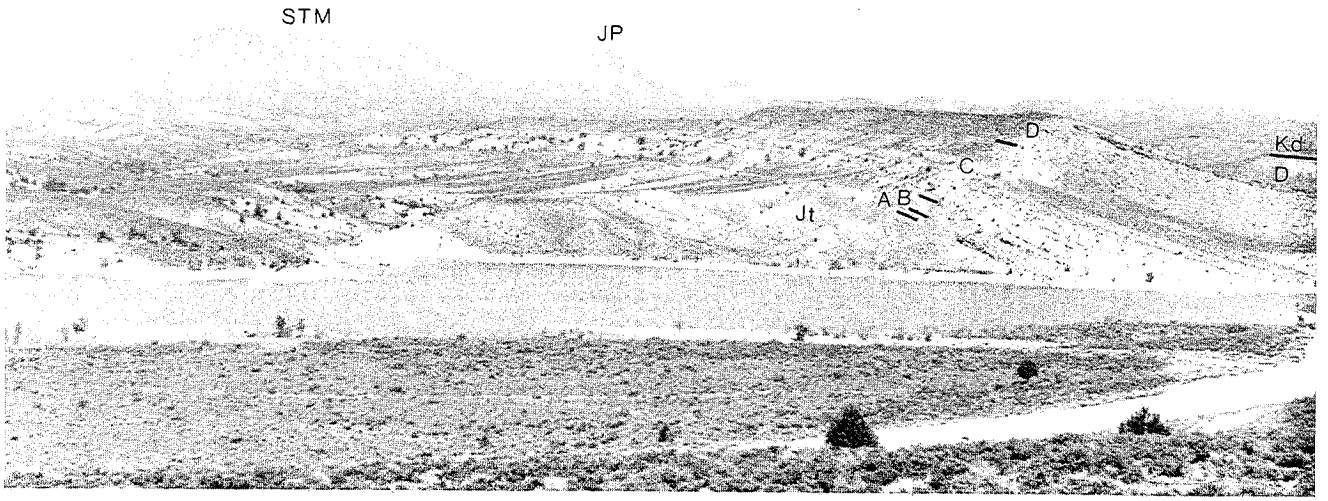

FIGURE 5.—*View northwest across Gunlock Reservoir toward Square Top Mountain (STM) and Jackson Peak (JP). The cuesta running from the Reservoir to Square Top Mountain is held up by Carmel strata. The letters A–D are approximately on line with measured section 7 and represent members within the Carmel Formation. The Carmel is bounded by Temple Cap Formation (Jt) below and Dakota(?) Conglomerate (Kd) above.*

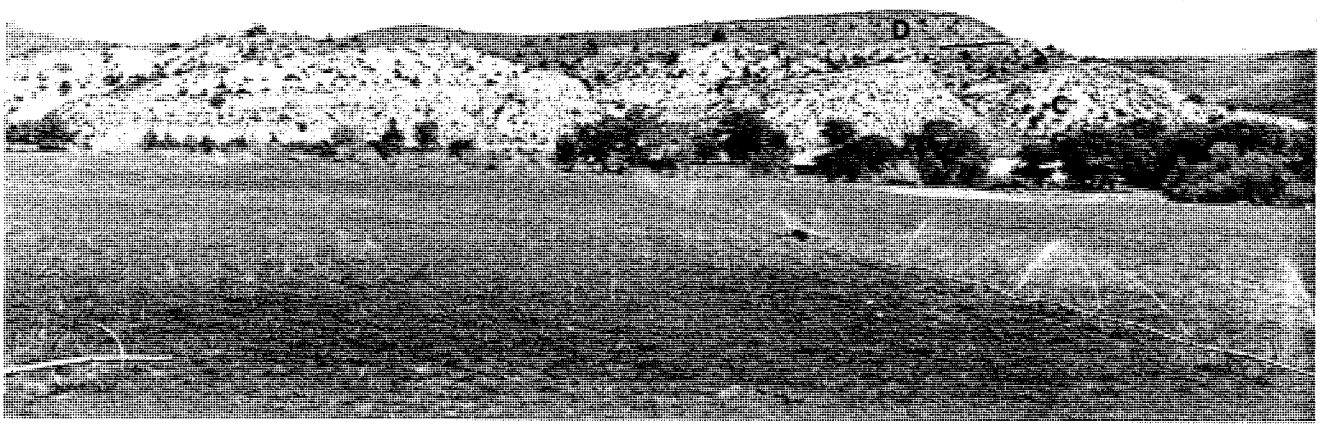

FIGURE 6.—*View northeast from the Gunlock-Veyo highway (seen in the extreme left of photo) to Carmel bluffs measured in section 9. The letters C and D represent members within the Carmel Formation. Members A and B are hidden behind trees in middle right-hand portion of photo.*

Co-op Creek Member of the Carmel Formation against white and reddish sandstone of the Cretaceous Iron Springs Formation.

The lower contact of the Carmel Formation has been mapped at the base of the lowest persistent limestone, above the gypsiferous red beds here included in the Temple Cap Formation (Hintze 1986). The 2-m-thick limestone is clearly identifiable along the cuesta face northeast of Manganese Wash (fig. 5), but thins to only 1.2 m north of Gunlock in section 9 and is obscured or faulted below valley fill along the Santa Clara River valley in section 10. Peterson and Pipiringos (1979) included the upper parts of underlying reddish beds, considered here within the Temple Cap Formation, as part of the lower limestone member. They showed the "J–2" regional unconformity of Pipiringos and O'Sullivan (1978) as separat-

ing these reddish gypsiferous mudstones from the underlying Temple Cap Sandstone in areas to the east. They continued this unconformity, even though poorly defined, westward above grossly similar red beds and gypsum of the Temple Cap Formation (fig. 3) in the Gunlock area (Voorhees 1978, p. 14, 125). If the J–2 unconformity does indeed split the apparently homogenous gypsiferous mudstones below the basal Carmel limestone, then these red beds below the limestones and above the "J–2" post-Temple Cap unconformity should be included within the Carmel Formation. I could not find an unconformity within the red-bed section and have placed the formation contacts at the red-bed–carbonate contact for purposes of convenience.

The upper boundary of the Carmel Formation is an unconformity below Cretaceous Dakota(?) Conglomerate. This relationship occurs throughout the study area, except near measured sections 2 and 9, where Cretaceous Iron Springs Sandstone is faulted against the Carmel, and near section 8, where Quaternary colluvium rests unconformably on the upper part of member D. The contact of the Carmel Limestone and the overlying Dakota(?) Conglomerate is a regional angular unconformity (Blakey and others 1983), but it is only locally disconformable in the Gunlock area (Wright and Dickey 1963a). The unconformity is well exposed along bluffs near the Santa Clara River north of Gunlock in section 15, T. 40 S, R. 17 W, where a conglomerate-filled channel of Dakota(?) is deeply entrenched into the upper part of the Co-op Creek Member (fig. 7). Variations in pre-Dakota(?) Conglomerate erosional depths are documented by differences in stratigraphic thickness of underlying (fig. 8, in pocket) Carmel strata, which range from 120 m in faulted exposures at section 10 to approximately 240 m in cuestas near sections 1a and 1b. The difference in thickness is a result of pre-Dakota erosion during an interval of nearly 80 million years (Hintze 1986). This variable erosional depth caused earlier workers, who measured the deeply truncated section near Gunlock Reservoir (section 7), to conclude that only part of the lower Co-op Creek Member was preserved in the Gunlock region.

Regional correlations between members of the Carmel Formation in southern Utah with the members of the Arapien Shale and Twin Creek Formation suggests that the Co-op Creek Member of the Carmel Formation is equivalent to the Sliderock and Rich Members of the Twin Creek Limestone of Imlay (1967) in northern Utah (Blakey and others 1983). Similarly, the Crystal Creek and Paria River Members of the Carmel are correlative to the Boundary Ridge and Watton Canyon Members of the Twin Creek Formation. The Gypsum Spring Member of the Twin Creek Limestone is thought to be equivalent to the Temple Cap Formation (Peterson and Pipiringos 1979). Imlay (1964) claimed that bivalves from the Twelve-Mile Canyon Member of the Arapien Shale in central Utah show that it is equivalent to the Twin Creek Limestone and Carmel Formation and ranges from Bajocian to Callovian.

DAKOTA(?) CONGLOMERATE

The Dakota(?) Conglomerate of Cretaceous age lies on various stratigraphic levels of the Carmel in the Gunlock area. Relief on the unconformity beneath the Dakota(?) amounts to more than 100 m within the study area (fig. 8, in pocket) and, according to Hintze (1986), represents an elapsed time of about 80 million years. Dakota(?) rocks are missing and the Iron Springs Formation is in fault contact with Carmel rocks in the central third of the study area.

The massive Dakota(?) Conglomerate ranges from 13 m thick near section 10 to only several centimeters thick near section 4b. A moderate red bentonite that contains walnut-sized barite nodules is present between the Dakota(?) Conglomerate and Iron Springs Formation everywhere in the study area. Zircons from the bentonite yielded a fission track age of 80 ± 10 Ma (Hintze 1986). Well-rounded quartzite and chert clasts constitute 70% of the conglomerate. They range up to 25 cm across but generally are 4 to 10 cm in diameter. Sandstone lenses up to 30 cm thick and 10 m across occur within the conglomerate but are rare. Calcareous sandstone matrix occupies the remaining rock volume. The conglomerate weathers to dark brownish black. Stokes (1952) concluded that Dakota(?) sands and gravels elsewhere accumulated in a complex braided stream environment on a pediment surface. Such may also be the environment of deposition here.

SEDIMENTOLOGY

The Carmel Formation can be divided into six members based on outcrop appearance and lithology. These members are herein labeled A through F in ascending order (fig. 8). Members A–D are part of the Co-op Creek Limestone Member of Doelling and Davis (1989). Member E is believed to be equivalent to the Crystal Creek Member and member F is believed to be equivalent to the lower Paria River(?) Member of Thompson and Stokes (1970). Figure 8 shows the ten measured sections and documents lateral and vertical facies relationships within the formation.

MEMBER A

Member A is a ledge-forming carbonate sequence that ranges from silty dolomitic lime mudstone, at the base, to an intensely ripple-marked, oolitic packstone at the top. Base of the member is at the Temple Cap–Carmel Formation boundary and is marked by the lowest recogniz-

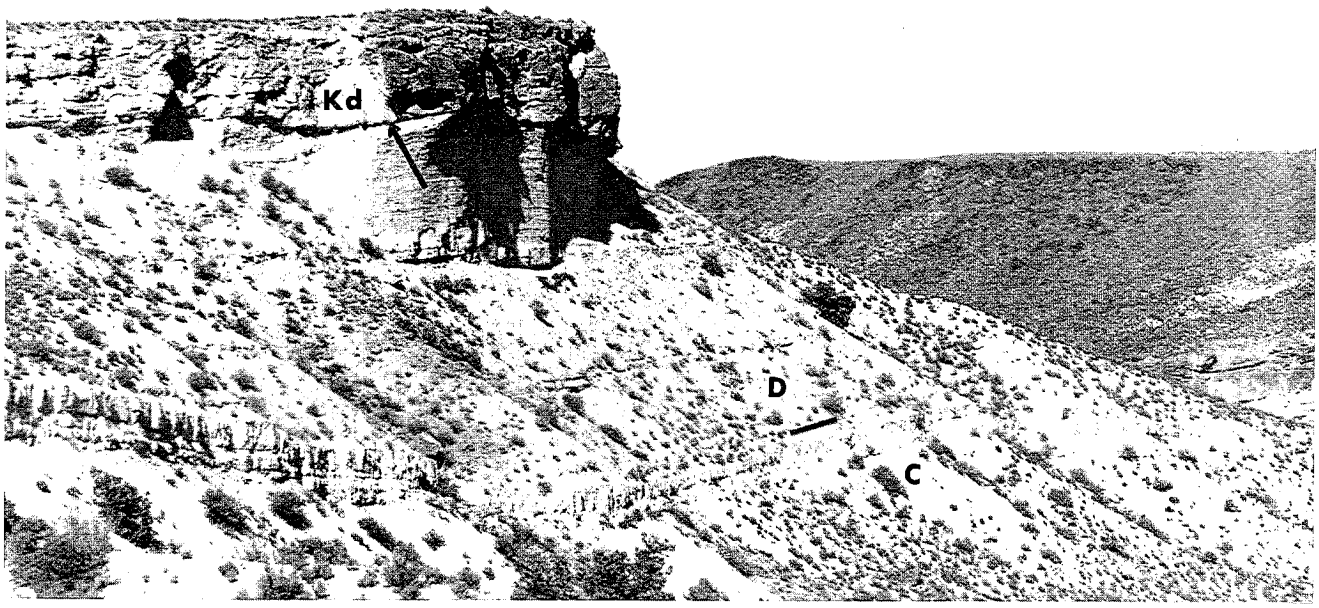

FIGURE 7.—*View northeast from the ranch road toward the upper part of measured section 10. Channel-filling Dakota(?) Conglomerate (Kd) unconformably caps bluffs of Carmel Formation (arrow). The letters D and C represent members within the Carmel Formation.*

able yellowish gray, ledge-forming carbonate above the reddish brown terrigenous, slope-forming Temple Cap Formation. A massive bed of gypsum (fig. 9), up to 5 m thick in some localities, occurs in the upper part of these reddish brown deposits. These rocks are well exposed near the base of the Carmel cuesta, northwest of Gunlock Reservoir, as seen in figure 5. Member A extends upward from this boundary ledge to slope-forming reddish brown mudstone. The member thins from 2.4 m thick in section 1a to 1 m in section 9 (fig. 8). Analysis of the measured sections indicates a general southwest to northeast thinning rather than truncation or facies changes at the base. Member A is not exposed in sections 8 and 10.

Dolomitic Lime Mudstone

Dolomitic lime mudstone forms the bottom half of member A. This rock is moderate yellow, thin bedded, slabby, and appears to be gradational from the underlying siltstones of the Temple Cap Formation. This basal Carmel unit contains abundant silt and sand. It grades upward into oolitic packstone. Organic activity was limited during deposition of the dolomitic lime mudstone; no fossil fragments nor bioturbation are evident.

Oolitic Packstone

Oolitic packstone makes up the top half of member A. This rock is yellowish gray, thin bedded, blocky, heavily pitted, intensely ripple marked, and cross-bedded. It is capped with a 5-mm-thick biotite rich siliceous rind. Oolites, gastropods, and bivalve fragments in the rind have been replaced by chalcedony and microcrystalline quartz (fig. 10).

This rock is directly overlain by the basal volcanic ash and siltstone of member B. These ashy clastic rocks probably served as the source for silica that replaced the upper carbonate grains and cement. Carbonate grains, though not replaced below the upper 5-mm-thick siliceous rind, are visibly altered and consist of fine- to medium-grained oolites and occasional immature gastropods and bivalve fragments. Spherical, perhaps windblown quartz grains account for less than 1% of the constituents.

Cavernous porosity, made of interconnecting pores up to 3 mm in diameter, produce 15%–20% total pore space. Early lithification, before compaction, probably resulted in preservation of primary porosity, which served as pathways for acidic solutions that formed the cavernous pores and for silicic solutions that later filled the upper pore spaces.

Straight-crested wave ripples occur on the surface of these packstones (fig. 11). These ripple marks reach 10 cm in amplitude and 20–30 cm in wave length and are best preserved in sections 1–4. The association of large wave ripples below volcanic material leads to conjectures that seichelike currents associated with distant volcanic eruptions shaped the upper surface of the shallow-water carbonates before they were buried by ash fall.

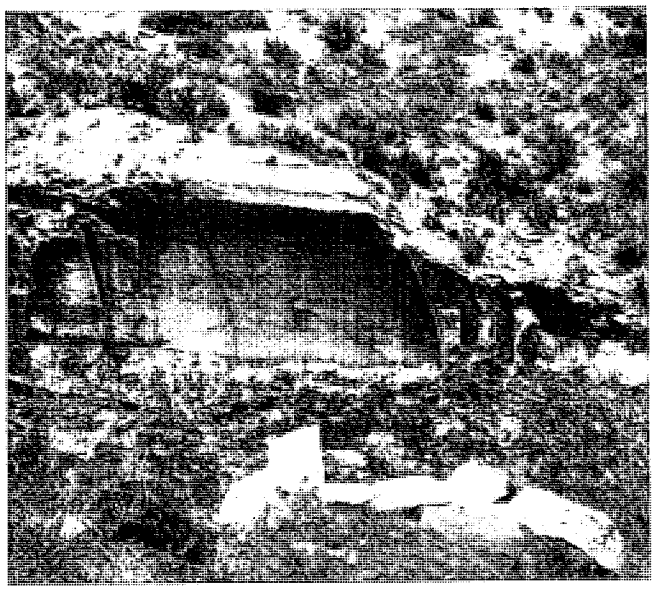

FIGURE 9.—*Massive gypsum in the Temple Cap Formation just below the Temple Cap–Carmel contact near section 9. Jacob's staff for scale, 1.5 m.*

FIGURE 10.—*Photomicrograph of silicified oolitic margin (bright white color) in upper unit 1, section 7. Bar is 2 mm long.*

MEMBER B

Member B is a slope-forming, terrigenous, and volcanics-rich sequence of rocks that extends from the top of member A to the base of the next ledge-forming carbonate in member C (fig. 5). Member B varies in thickness from 12.7 m in section 1a to 8.6 m in section 6 and generally thins in a northwest to southeast direction (fig. 8). Member B becomes increasingly gypsiferous toward Diamond Valley, where massive gypsum units range up to 1 m thick in exposures in the southwest quarter of section 1, T. 40 S, R. 16 W, 14 km east of Gunlock. Member B is covered in section 8 and 10 by valley fill. Member B consists of two rock types: a siltstone to mudstone unit sandwiched between volcanic ashes.

Siltstone-Mudstone

Siltstone to mudstone beds make up the middle 6–10 m of member B. It is moderate reddish brown, laminated, slope forming, and composed of subangular feldspar and quartz silt with scarce biotite grains. Vugs lined with calcite crystals, possibly after gypsum, suggest a period of arid and hypersaline conditions. Body fossils, trace fossils, and bioturbation are absent.

Volcanic Ash

Pale green volcanic ash constitutes the upper 2.5 m and the lowest 1.5 m of member B. These horizons are labeled ashes AA and A in column 1a of figure 8. They are composed of thin-bedded pale green clay and unconsolidated feldspar, and quartz silt. Black biotite grains in Ash A, as much as 2 mm in diameter, generally lie parallel to bedding and are evenly distributed within the surrounding matrix. Biotite accounts for 5%–10% of the volume. Heavy minerals include traces of zircon, sphene, apatite, and Fe-Mg minerals. Schultz and Wright (1963) chemically analyzed samples selected from bentonitic layers in the Carmel throughout Utah, including a sample that appears to have been taken from ash A in the Gunlock area. Their results indicate that the bentonites range from dominantly montmorillonite to kaolinite and illite.

MEMBER C

Member C is a ledge-forming carbonate sequence with scattered slope-forming terrigenous siltstone and volcanic ash units. Member C consists of four cycles. Each cycle generally includes, from bottom to top, an oolite grainstone-packstone, lime mudstone-wackestone, intraclastic packstone, algal stromatolite, volcanic ash, and siltstone (fig. 8). Evaporite solution breccia and sandstone also is present in some cycles. Member C ranges in thickness from 76 meters in section 1a to 65 meters in section 7. Alluvial cover in section 8 buries members A, B, and the lower two thirds of C. Analysis of the measured sections shows a northwest to southeast thinning of member C. The lower third of the member becomes increasingly gypsiferous eastward in exposures in Diamond Valley, similar to that described in member B.

The lower contact of member C was placed at the base of the first ledge-forming carbonate above the slope-forming, pale green ash and moderate reddish brown mudstones of member B (fig. 5). The upper contact of member C was placed at the top of the upper ledge-forming, yellowish gray, algal stromatolite bed below slope-form-

FIGURE 11.—*Straight-crested wave-ripples, unit 2, section 2. Hammer head for scale.*

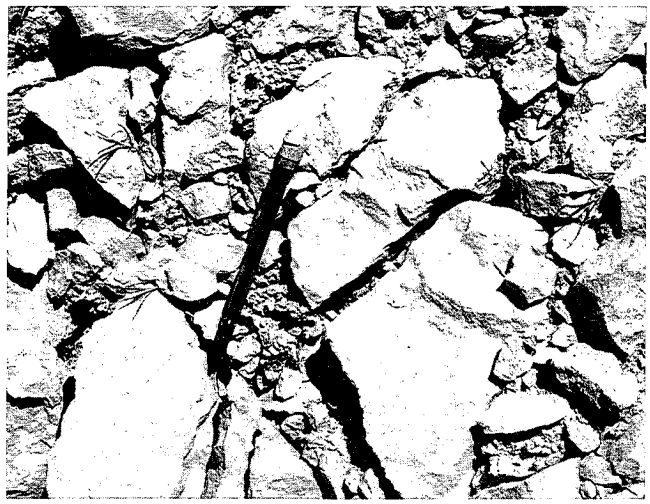

FIGURE 12.—*Yellowish gray, flat, subrounded, muddy intraclasts surrounded by yellowish brown oolitic material, unit 49, section 10. Pencil for scale.*

ing, pale olive brown, oolitic-rich siltstone of member D. This transition is midway up cuesta fronts near Gunlock Reservoir, as shown in figure 5. The same sequence is exposed in sections 9 and 10.

Oolite Grainstone-Packstone

Oolite grainstones to packstones occur as ledges that make up 5% of member C. They are distinguished from other rock types in the field by their oolites and siliceous, rusty-appearing, dark yellowish orange weathering color. Oolite grainstone units, in member C, are 0.5 m thick and underlie massive lime mudstone and wackestone. An unusual sequence of fluted oolite packstone is located in the upper third of member C in sections 9 and 10. These isolated sequences contain undulatory small current ripples, flute casts, and herringbone cross-bedding.

Oolite grainstones to packstones contain fine- to medium-grained oolites with minor amounts of echinoderm, bryozoan, and bivalve fragments. Oolite nuclei are bioclasts, fecal pellets, and occasionally quartz silt. Compound oolites and grapestones also occur. Numerous yellowish gray, flat, subrounded concretions, 2–3 mm in diameter, occur on bedding plane surfaces (fig. 12). *Pentacrinus* columnals as well as bivalve fragments differentially weather out on rock surfaces. A small coral colony 2 cm in diameter was found on the surface of unit 34, section 9 (fig. 13B).

Lime Mudstone-Wackestone

Ledge- and cliff-forming lime mudstone to wackestone accounts for 60% of member C. Lime mudstone and wackestone rock types are combined here because they represent similar low-energy environments and grade into each other in the field. Wackestones in member C occur within thicker beds of similar-appearing lime mudstone.

Lime mudstone to wackestone units are yellowish gray, laminated, and form the base of the thick resistant "stair steps" midway up the Carmel cuestas northwest of Gunlock Reservoir (fig. 5). These rocks also form the base of ledges midway up faulted exposures northeast of Gunlock (fig. 6). Lime mudstones fracture easily and form slopes covered with pencil-shaped fragments. Much of this rock type is argillaceous and forms less resistant, ledgy slopes.

The lime mud is interlaminated with wispy lenses of ostracodes, quartz silt, and scattered calcitized gypsum crystals (fig. 14A). Most of the lime mudstone to wackestone units grade upward into algal stromatolites and may also have algal origins. Miliolid foraminifers, oolites, radiolarians(?), and fragments of bryozoans, crinoids, ostracodes, and bivalves were observed in thin section (fig. 14B–D). Shallow-water wave ripples of oolitic grainstone to packstone are preserved within uppermost lime mudstones of member C (fig. 15).

Intraclastic Packstone

Intraclastic packstone constitutes 1% of member C. These rocks are light olive gray, thin-bedded, slabby, ledge formers that fill channels cut into lower units. Unit 24, section 7, is typical of this rock type. Medium- to very coarse-grained lime mudstone intraclasts make up 80% of the grains (fig. 16), whereas bivalve, bryozoan, gastropod, crinoid, and ostracode fragments, intermixed with oolites and botryoidal-shaped grapestones, constitute the remainder.

Algal Stromatolite

Algal stromatolites cap the resistant ledges midway up the Carmel cuestas northwest of Gunlock Reservoir as well as the faulted exposures northeast of Gunlock. Ten percent of member C is composed of algal stromatolite.

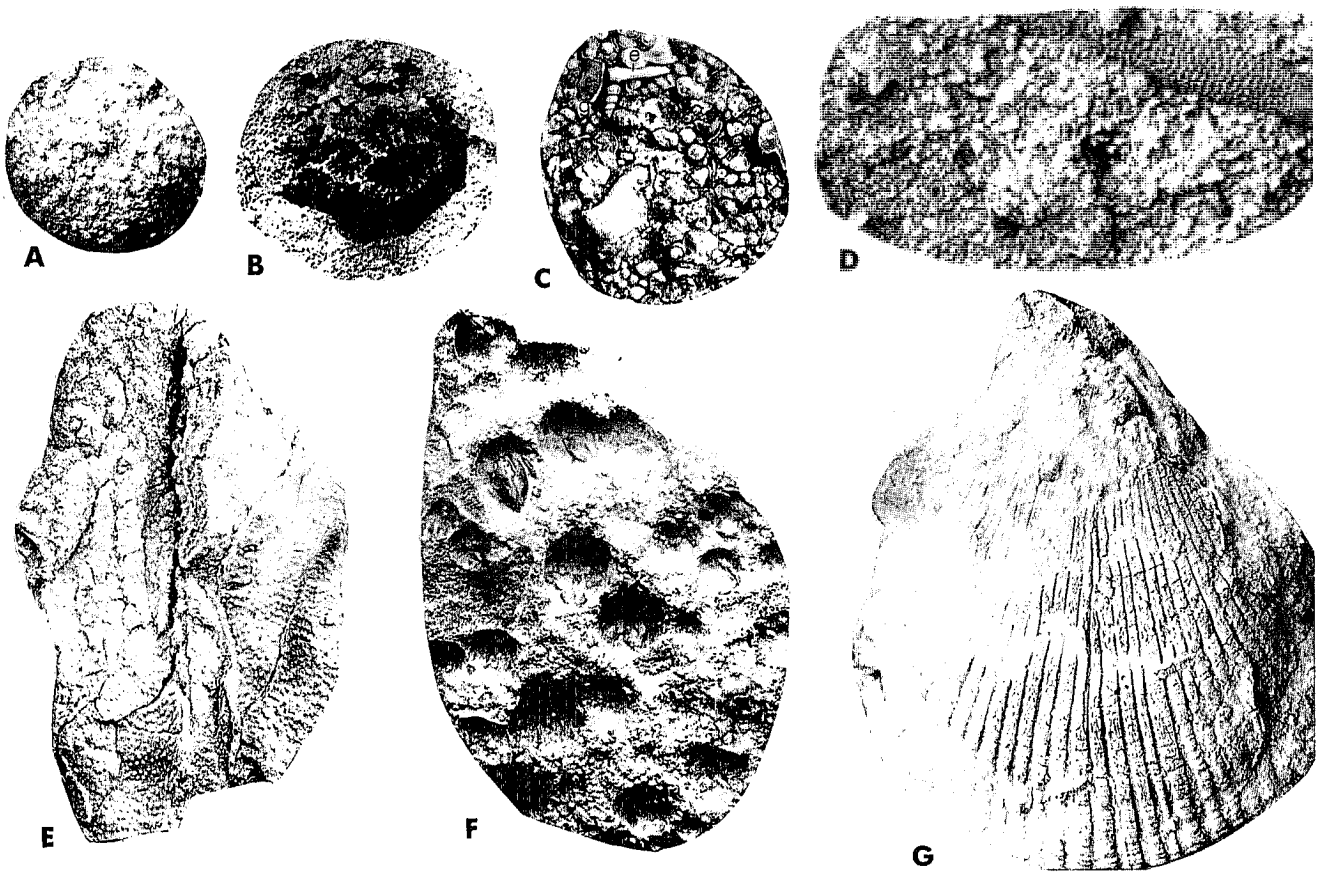

FIGURE 13.—*(A) Regular echinoid from section 10, unit 56, X3 (BYU 4001). (B) Colonial coral,* Astrocoenia *Milne Edwards and Haime (?), section 9, unit 34, X3 (BYU 4002). (C) Echinoid spine (e) and turreted gastropods (g) with oolites and echinoderm debris, section 8, unit 27, X3 (BYU 4003). (D) Large echinoid spine in the upper right and a* Pentacrinus *columnal in upper left mixed with oolites and echinoderm debris, section 9, unit 34, X2.5 (BYU 4004). (E) Cyclostome bryozoan, section 10, unit 56, X1.6 (BYU 4005). (F) Bivalve-inhabited bored hardgrounds, section 8, unit 32, X1.6 (BYU 4006). (G)* Lima (Plagiostoma) occidentalis *Hall and Whitfield, section 10, unit 56, X1 (BYU 4007).*

Two types were distinguished, based on classification of Recent stromatolites by Logan and others (1964) in Australia: a discrete vertically stacked (SH) columnar type (fig. 17A), and a laterally linked hemispheroid (LLH) type (fig. 17B).

Columnar stromatolite was found in a 1.3-m-thick bed (unit 29 of section 10) that is well exposed in section 10. The unit thins southwestward and pinches out before it reaches sections measured near Gunlock Reservoir. The stromatolite columns are dolomitic, generally 3 cm in diameter, and are separated by 0.5-cm-thick, calcite-filled porous zones. Dolomitization of the individual columns and interspaces probably occurred soon after deposition and before replacement of the interstitial debris. The columnar stromatolite rests upon an evaporite solution breccia.

The most common algal stromatolite in member C is the LLH type. This type is yellowish gray, argillaceous, and forms wavy-laminated packages, 0.5–1.5 m thick. It caps resistant shoulders midway up the Carmel cuestas north of Gunlock Reservoir. In general, the stromatolite's upper contact is sharp, but the lower is gradational from cryptalgalaminate below. The stromatolites become more argillaceous upward, and intensely mudcracked bedding planes are common. Small-current ripples, selenite crystal casts, raindrop impressions, and parting lineations are associated with these argillaceous partings (fig. 17C–D).

Small, bubblelike calcitized gypsum rosettes, 0.5–1 cm in diameter, occur at midthickness in the stromatolite packages. The quantity of rosettes increases upward until the top surface of some stromatolites are entirely covered with a thin glistening layer (fig. 17D–E). These layers are

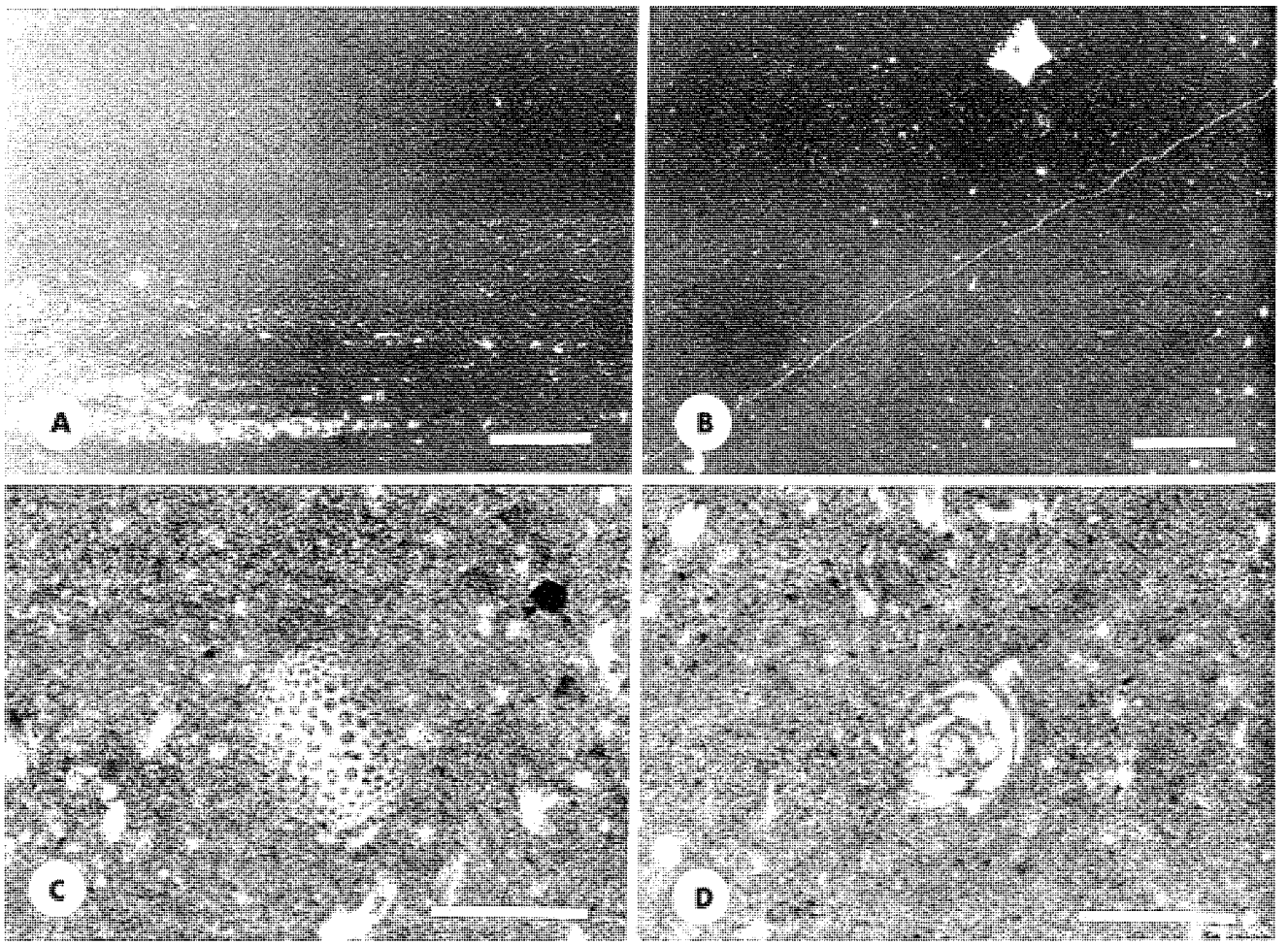

FIGURE 14.—*(A) Photomicrograph of lime mudstone with scattered silt, ostracode valves, and small peloids, section 9, unit 38. Bar is 2 mm long. (B) Photomicrograph of lime mudstone with* Pentacrinus *columnal and scattered silt, section 10, unit 17. Bar is 2 mm long. (C) Photomicrograph of a siliceous radiolarian(?) in lime mudstone, section 9, unit 16. Bar is 0.2 mm long. (D) Photomicrograph of a miliolid foraminifer in lime mudstone, section 10, unit 14. Bar is 0.2 mm long.*

especially characteristic of stromatolites in upper member C. Undulatory lime mudstone laminae and iron-stained filaments (?) formed by original trapping algae are interspersed with quartz silt and calcitized anhydrite casts, 0.25 mm long. Algal stromatolites are typically bounded above by terrigenous mudstones. These stromatolites are similar to most fossil algal mats in that the original algal filaments are not preserved. The absence of recognizable filaments in most ancient stromatolites is probably due to collapse of algal filaments upon desiccation (Aitken 1967).

Evaporite-Solution Breccia

Evaporite-solution breccia forms a 20-cm-thick, reddish yellow ledge in member C. It is thickest in sections 9 and 10 and thins southwestward to less than 10 cm in section 7. Angular dolomitic fragments, 0.5–1 cm across, are chaotically oriented in a calcite cement (fig. 18) heavily pockmarked with small masses of chalcedony. Dissolution of gypsum interbedded within semilithified carbonate mud resulted in their collapse and angular fragmentation. Later calcification and silicification have recemented the clasts. The thinness of the unit, as well as visible remnant bedding, suggest that the remaining fragments were only displaced several millimeters from their original position.

Volcanic Ash

Pale green volcanic ash accounts for 5%–10% of member C in three slope-forming horizons labeled ashes B, C, and D in column 1a of figure 8. These ashes are similar to the ashes of member B and range from 10% to less than 1% biotite. Ash B is thickest and most easily recognized. Ashes C and D generally appear as broad soily slopes, yet are excellently exposed in roadcuts at section 8.

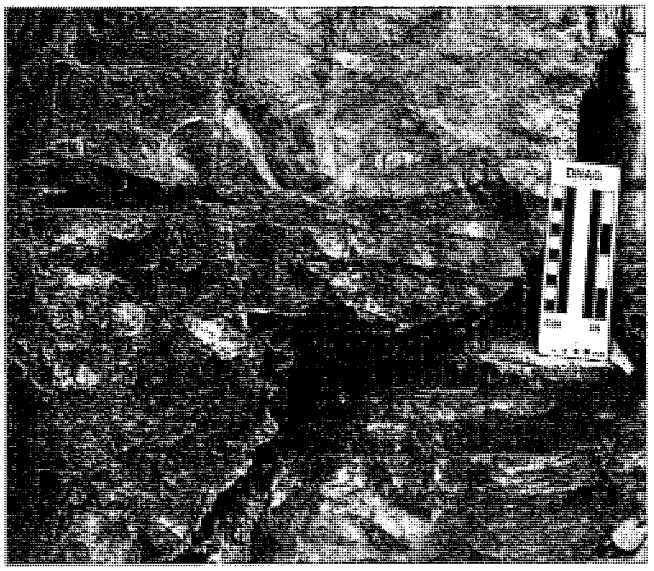

FIGURE 15.—*Wave ripples of oolitic packstone sandwiched between lime mudstone, unit 33, section 1a.*

Sandstone

Only one sandstone unit was recognized in member C along measured sections 6, 7, 9, and 10. It changes westward to a siltstone. The unit thins northeastward from 3 m in section 7 to only 1.5 m in sections 9 and 10. It is a grayish yellow, medium-bedded, well-sorted, subangular, and fine-grained oolite-feldspar-quartz sandstone that weathers into spheroidal blocks and outcrops (fig. 19).

Oolites, marine bioclasts, and lithoclasts constitute 10% of the grain, feldspar fragments 13%, and quartz sand makes up the remainder. The presence of evaporites such as large, sucrosic, calcitized gypsum vugs in the sandstone in section 9 and several 10-cm-thick lenses of open-marine, oolite-grainstone units interbedded within the same sandstone horizon in section 7 suggest that marine conditions prevailed to the west and nonmarine conditions to the east.

Siltstone-Mudstone

Medium- to fine-grained clayey quartz siltstone and mudstone constitute 10% of member C. Rare horizons of lime siltstone also are present. Slope-forming siltstones and mudstones range from pale yellowish orange to light olive gray. In fresh exposures, the siltstone weathers into small, 0.1–5 cm-sized polygonal chips. Excellent ripple-marked siltstone exposures occur in recently exposed undercut banks above the Santa Clara River in section 10.

Gypsum beds, 0.5 cm thick, occur in lower siltstone units of member C in section 10. Residual biotite grains, probably reworked from adjacent volcanic ashes, are common on surfaces of siltstone bedding planes.

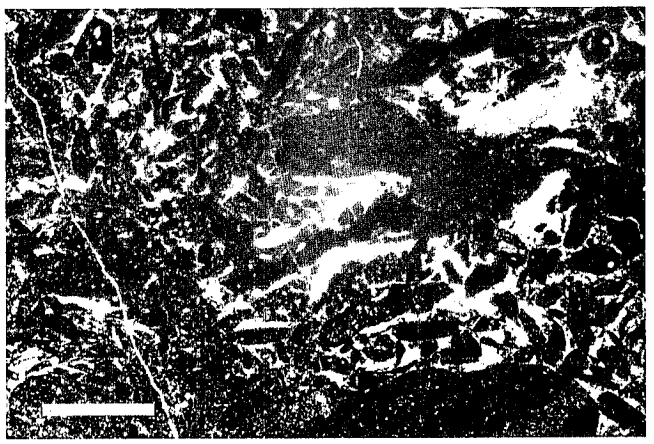

FIGURE 16.—*Photomicrograph of intraclastic packstone, unit 24, section 7. Bar is 2 mm long.*

MEMBER D

Member D is a single 70-m-thick, shallowing-upward carbonate sequence similar to the four smaller cycles in member C. Member D contains interbedded, ledge-forming, sandy-oolite grainstone and slope-forming lenticular-bedded oolite-siltstone. Intraclastic-fossiliferous packstone, argillaceous lime mudstone, terrigenous mudstone, and oyster boundstone also occur in lesser amounts. Slope-forming, terrigenous mudstones in member D occupy the same position in the depositional sequence as do lime mudstones to wackestones in depositional cycles of member C. The lower contact of member D was placed at the top of the highest algal stromatolite in member C and below major slope-forming siltstone at the base of member D. This transition occurs midway up the Carmel cuestas, northwest of Gunlock Reservoir as seen in figure 5. The same sequence is exposed midway up faulted exposures northeast of Gunlock (fig. 6).

The upper contact of member D was placed below the first moderate reddish brown siltstone in member E and above the last lime mudstone and stromatolite sequence of member D. This boundary is exposed in sections 3b, 4b, and 7. Elsewhere, pre-Dakota(?) erosion and/or subsequent faulting has eliminated Carmel exposures above the middle part of member D (fig. 8).

Oolite-Siltstone

Pale yellowish orange, slope-forming, oolite-rich terrigenous siltstone makes up 37% of member D and forms broad dip slopes behind the Carmel cuestas north of Gunlock Reservoir. Rippled lenses of fine-grained oolite sands and silts, 1–5 mm thick, are sandwiched between thicker layers of weakly consolidated, muddy, quartz silt. Adjacent slopes are often covered with rippled oolite flakes and chips, up to 7 cm across, that weather out from the surrounding siltstone. Oolite grainstone beds, up to

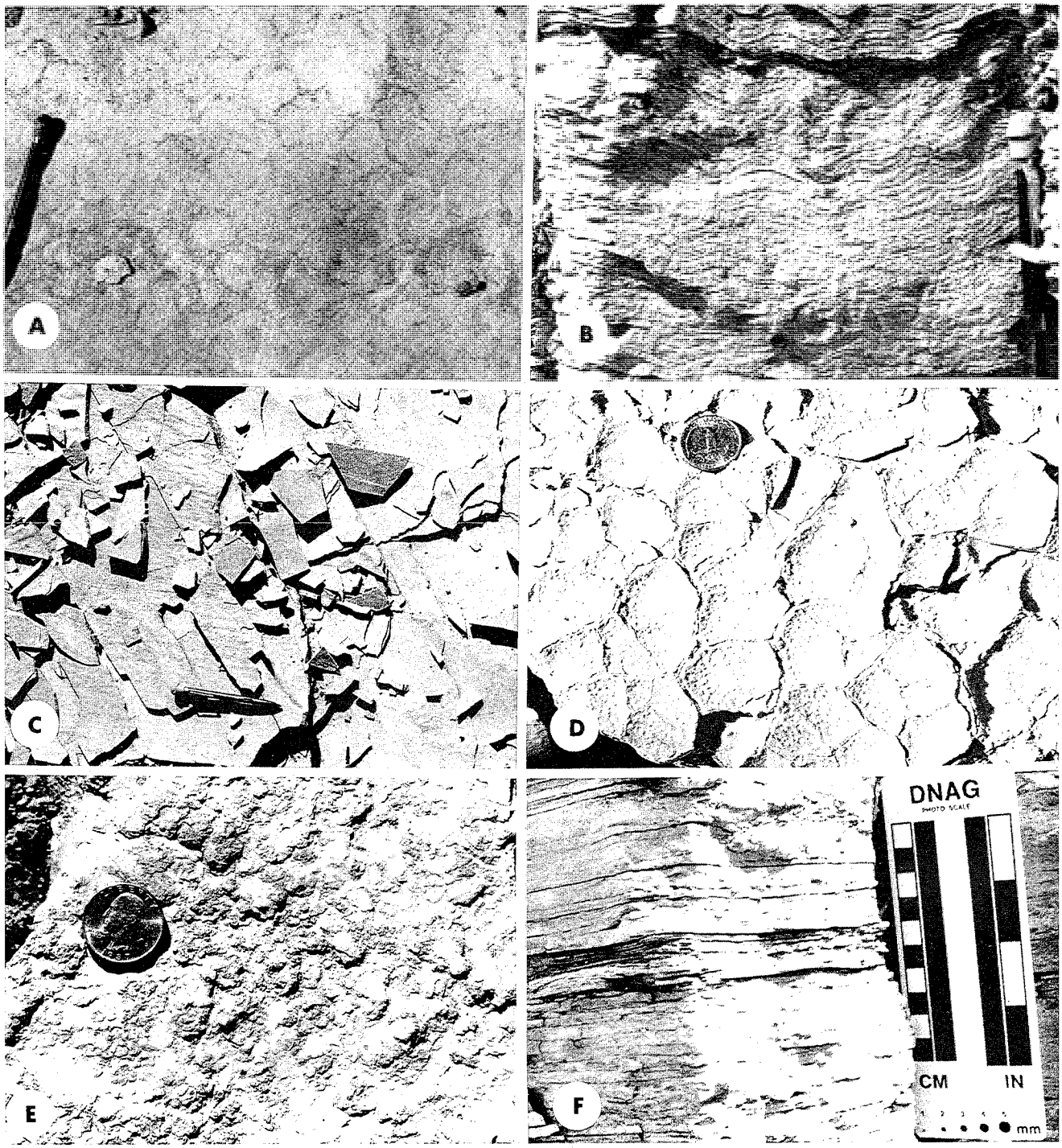

FIGURE 17.—*(A) Plan view of vertically stacked columnar stromatolites, unit 29, section 10. (B) Side view of laterally linked hemispheroidal stromatolites, unit 25, section 10. (C) Plan view of parting lineations trending north–south along the length of pencil, unit 41, section 10. (D) Plan view of dessication-cracked mudstone surface with raindrop impressions, unit 25, section 10. (E) Plan view of bubblelike, calcitized gypsum nodules that increase upward in unit 39, section 10, until they completely cover the top surface of the unit. (F) Side view of bubblelike calcitized gypsum nodules midway up unit 39, section 10.*

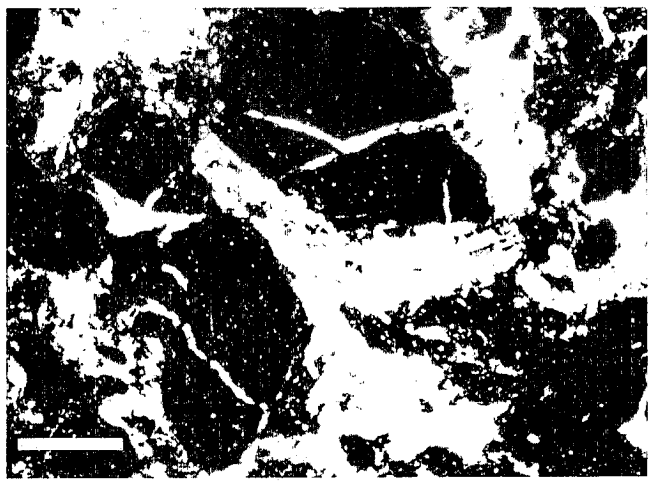

FIGURE 18.—*Photomicrograph of evaporite-solution breccia, unit 28, section 10. Most of the calcite cement has been replaced by chalcedony. Bar is 2 mm long.*

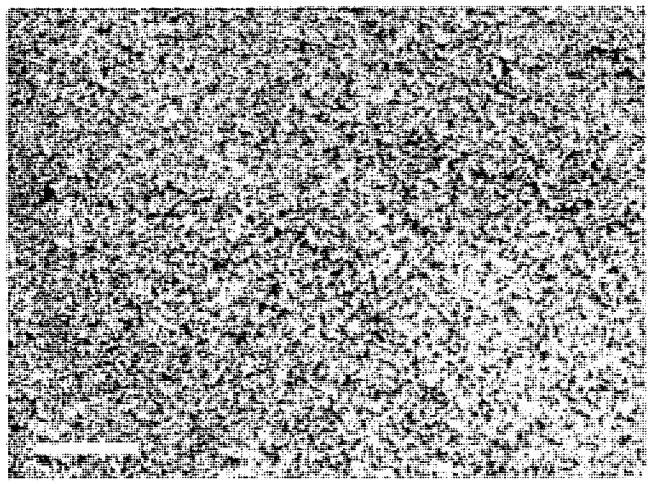

FIGURE 19.—*Photomicrograph of oolite-feldspar-quartz sandstone, unit 13, section 7. The small dark-colored circular grains are oolites. Bar is 2 mm long.*

10 cm thick, containing high-spired gastropods, oysters, and *Pentacrinus* fragments, are often interbedded in the siltstone. Trace fossils are commonly preserved on the undersides of rippled units (fig. 20A).

Sandy-Oolitic Grainstone

Sandy-oolitic grainstone accounts for 20% of member D. These rocks are pale yellowish orange, medium bedded, and hold up the Carmel cuestas north of Gunlock Reservoir. They also form ledges below the Dakota(?) Conglomerate in section 10. These rocks often have rusty brown siliceous crusts.

Medium-grained oolites account for 50%–70% of the allochems, quartz sand 20%–40%, and various fossil fragments the remainder (fig. 21). Oolite nuclei are peloids, bioclasts, quartz silt, and occasionally silt-sized oolites. Compound oolites and grapestones occur in some horizons. Fine-grained quartz grains differentially weather out in relief on grainstone surfaces and give the rock a misleading sandstone appearance. Some units contain large quantities of quartz sand lenses interbedded with oolite lenses (fig. 22). However, only one quartz sandstone bed, 0.6 m thick, occurs in member D. It is near the base of the member and, except for its light yellowish gray color, appears similar to oolitic grainstones. Fossil fragments consist of disarticulated bivalves, *Pentacrinus* columnals, and high-spired gastropods. Lower-spired gastropods, as well as bryozoan and ostracode fragments, are seen in thin section. Trace fossils occur on most bedding surfaces (fig. 20B–C).

Beautiful cross-bedded exposures and rippled surfaces (fig. 23A–F) exist in grainstones that hold up cuestas north of Gunlock Reservoir, as well as in grainstones capping the Carmel sequence northeast of Gunlock.

Mudstone

Slope-forming, light olive gray mudstone constitutes 40% of member D. It is calcareously cemented, yet weakly consolidated, and weathers into polygonal chips 0.5 cm across. It is well exposed in units near the top of section 7, where it surrounds subspherical oyster colonies.

Oyster Boundstone

Pale yellowish brown oyster boundstone occurs in 3 to 4, laterally traceable, 10–40-cm-thick ledges toward the top of member D. Erosion and/or faulting have removed part or all of these horizons from sections 1, 2, 3, 8, 9, and 10. Oyster boundstone is made of subspherical accumulations of *Ostrea* valves ranging from 10 cm to 2 m in diameter. These subspherical balls contain mature oysters intensely overgrown by juveniles. In most cases, juvenile oysters coat the balls with no preferred growth direction. In some locations, disk-shaped oyster masses occupy hardgrounds on fossiliferous packstones. This relationship occurs midway up section 5 in the NW 1/4, section 30, T. 40 S, R. 17 W, in the Gunlock Quadrangle. Local Gunlock residents have collected many of these oyster balls for their rock gardens (fig. 24).

Intraclastic-Fossiliferous Packstone

Ledge-forming, pale orange, thin-bedded, intraclastic-rich, fossiliferous packstone occurs in a few horizons within member D. This rock is made of a variety of bioclastic debris cemented by lime mudstone matrix (fig. 25). Oolites and quartz sand are rare. Bioclasts include oysters, bryozoans, *Pentacrinus* columnals, and echinoids (fig. 13A). Shell fragments of other bivalves, gas-

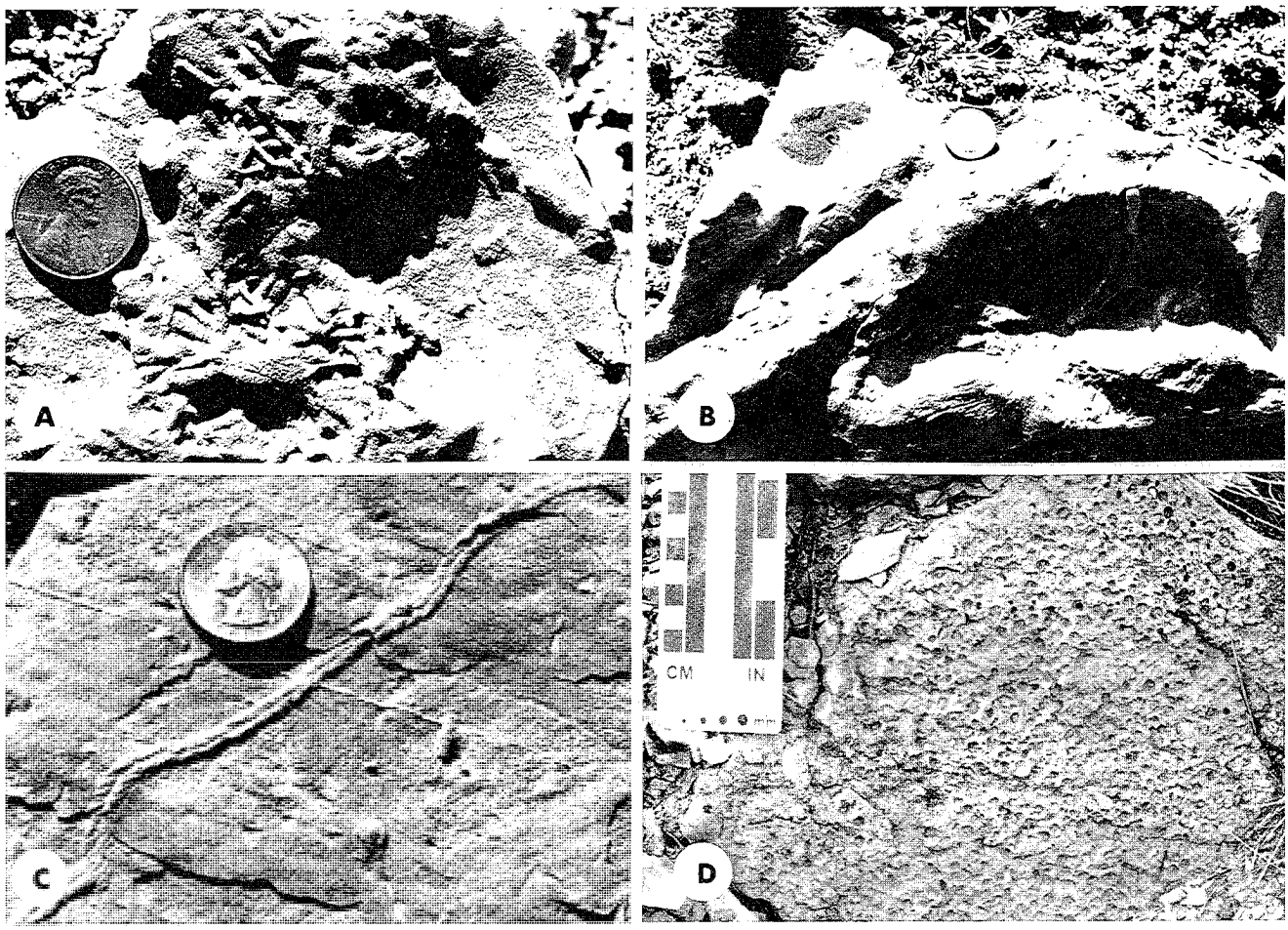

FIGURE 20.—*(A) Intrastratal, unilobate feeding structures on the underside of lenticular-bedded oolite grainstone chips, unit 26, section 8 (BYU 4008). (B) Unusually large trailway, unit 39, section 1a (BYU 4009). (C) Sinuous, bilobate-ridged, crawling trail with obliquely placed transverse pads, unit 53, section 10 (BYU 4010). (D) Plan view of bored hardgrounds, unit 56, section 5.*

tropods, and ostracodes are seen in thin sections. Bored hardgrounds occur in this rock type. They are particularly well exposed in gully exposures midway up section 5 below oyster colonies described above (fig. 20D). In rare cases, bivalves in growth position still remain within individual borings (fig. 13F). These hardgrounds provided ideal substrates for benthic organisms.

A layer of fossiliferous packstone fills channels cut into siltstone below Dakota(?) Conglomerate-capped bluffs in unit 56, section 10 (fig. 26). This is the same unit where echinoids and bryozoans were found.

Argillaceous Lime Mudstone

Thin-bedded, yellowish gray, argillaceous, lime mudstone is at the top of member D below moderate reddish brown siltstone of member E. There, light olive gray, terrigenous mudstone grades upward into platy, argillaceous lime mudstone that contains external molds of halite hopper crystals (fig. 27). Exposures of this vertical relationship are on the west flank of Limekiln Wash in section 4b. There, the uppermost 1.5-m-thick lime mudstone unit, below member E, becomes undulatory and stromatolitic upward. Erosion and faulting has cut and removed some or all of rocks equivalent to this bed from sections 1, 2, 8, 9, and 10.

MEMBER E

Member E is a dusky red siltstone, mudstone, and sandstone sequence interbedded with pale green volcanic ash. Its lower boundary was placed at the top of the highest occurrence of argillaceous lime mudstone in member D and at the base of the lowest occurrence of dusky red mudstone in member E. Its upper boundary was placed at the top of the highest slope-forming siltstone in member E and just below the cliff-forming carbonate sequence in member F. Normal faults in Limekiln and Manganese Washes have isolated exposures of member E in small cuestas eastward from the large cuestas

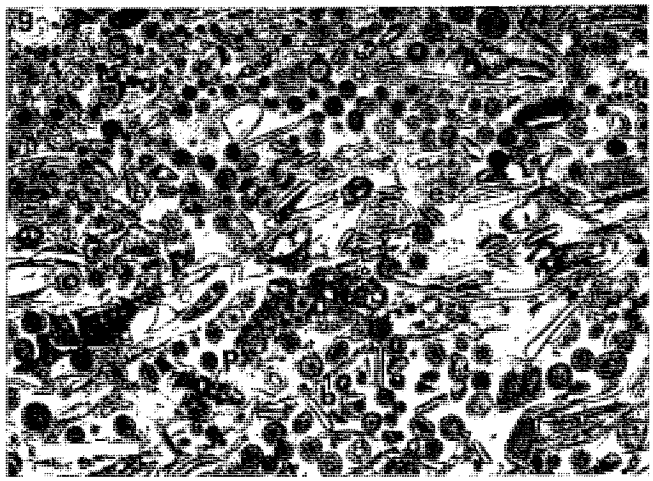

FIGURE 21.—*Photomicrograph of fossiliferous oolitic grainstone, unit 45, section 9. The unit contains numerous oolites and thinly coated bivalve fragments, gastropods (g), echinoderm fragments (e), bryozoans (b), and grapestones (p). Many oolite nuclei are made of quartz silt and sand. Bar is 2 mm long.*

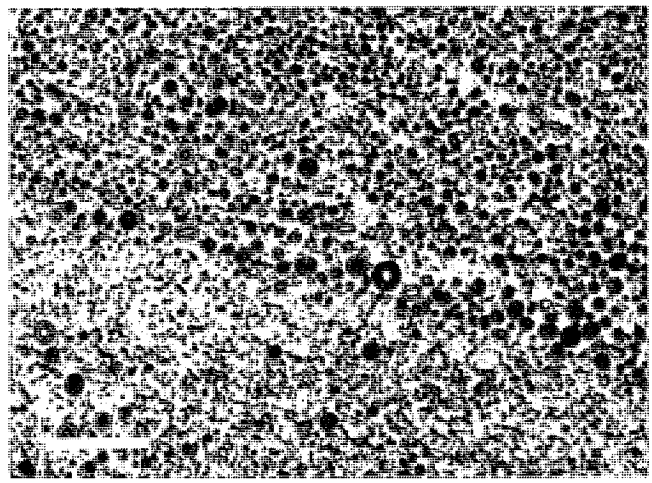

FIGURE 22.—*Photomicrograph of sandy-oolitic grainstone, unit 43, section 5. Note the distinct bedding boundary between predominantly oolite material and that of quartz silt and sand. Bar is 2 mm long.*

containing the lower portions of the Carmel seen in figure 5 (fig. 28). The most complete section of member E is in section 1b and is 48.5 m thick. Sections 3b, 4b, and 7 contain only parts of lower member E. All other sections lack rocks of member E owing to pre-Dakota(?) erosion and/or subsequent fault displacement (fig. 8). No fossils were seen in the member. Member E consists of 80% siltstone-mudstone, 15% sandstone, and 5% volcanic ash.

Siltstone-Mudstone

Thin-bedded, slope-forming, dusky red, quartz siltstone and mudstone dominate in member E. Subrounded to subangular quartz silt constitutes 60% of the particles and iron-stained clay the remainder. Thick, blocky calcite cement (fig. 29) constitutes 40% of the rock volume and probably formed by laterally wicking of calcium carbonate saturated waters in an evaporative setting. A thin-bedded, grayish yellow siltstone bed, 4.4 m thick, occurs at the top of member E in section 1b below the lowest carbonate bed of member F.

Sandstone

Two thin beds of moderate orange pink sandstone are also present in member E. The sandstone is well sorted and medium grained; it consists of 90% quartz grains (fig. 30) and 10% feldspar, chert, and lithic grains. The sandstone was differentiated from siltstone in the field by estimates of its mean grain size as well as by its ledge-forming nature and lighter color.

Volcanic Ash

Ledge-forming, pale blue green volcanic ash occurs in two, 1–1.5-m-thick beds in member E labeled ashes E and F in column 1b of figure 8. These two ashes are mineralogically similar to the older ashes of members B and C. Ash E is well lithified and calcareous. It contains 10% biotite and is an excellent marker bed for lateral correlation. The biotite grains are dark black and 1–2 mm in diameter. Ash F is more clayey, contains 1%–5% biotite, and is only preserved in section 1b.

MEMBER F

Member F is a 36-m-thick, fractured, cliff-forming, lime mudstone sequence. It is only preserved under Dakota(?) Conglomerate in section 1b. Elsewhere, the member has been removed by pre-Dakota(?) erosion and/or subsequent faulting (fig. 8). Section 1b is less than one mile from where Cretaceous age thrust faulting has displaced Permian allochthonous material, which makes up Square Top Mountain and Jackson Peak, over the Carmel and the other Mesozoic units below (fig. 31).

The lower boundary of member F was placed at the top of the highest occurrence of slope-forming siltstone in member E and below the lowest cliff-forming carbonate in member F. The upper boundary was placed at the top of the carbonate sequence at the base of the Dakota(?) Conglomerate. Member F rocks are similar to lime mudstones and wackestones of member C. Well-preserved calcitized gypsum crystal casts are common (fig. 32).

The upper half of member F is fractured and microfaulted. Fluids that filtered into the member along these fault and fracture planes have altered the rocks to a mottled reddish pink color. A single altered, though vaguely discernible, *Pentacrinus* columnal was found. Blocky cal-

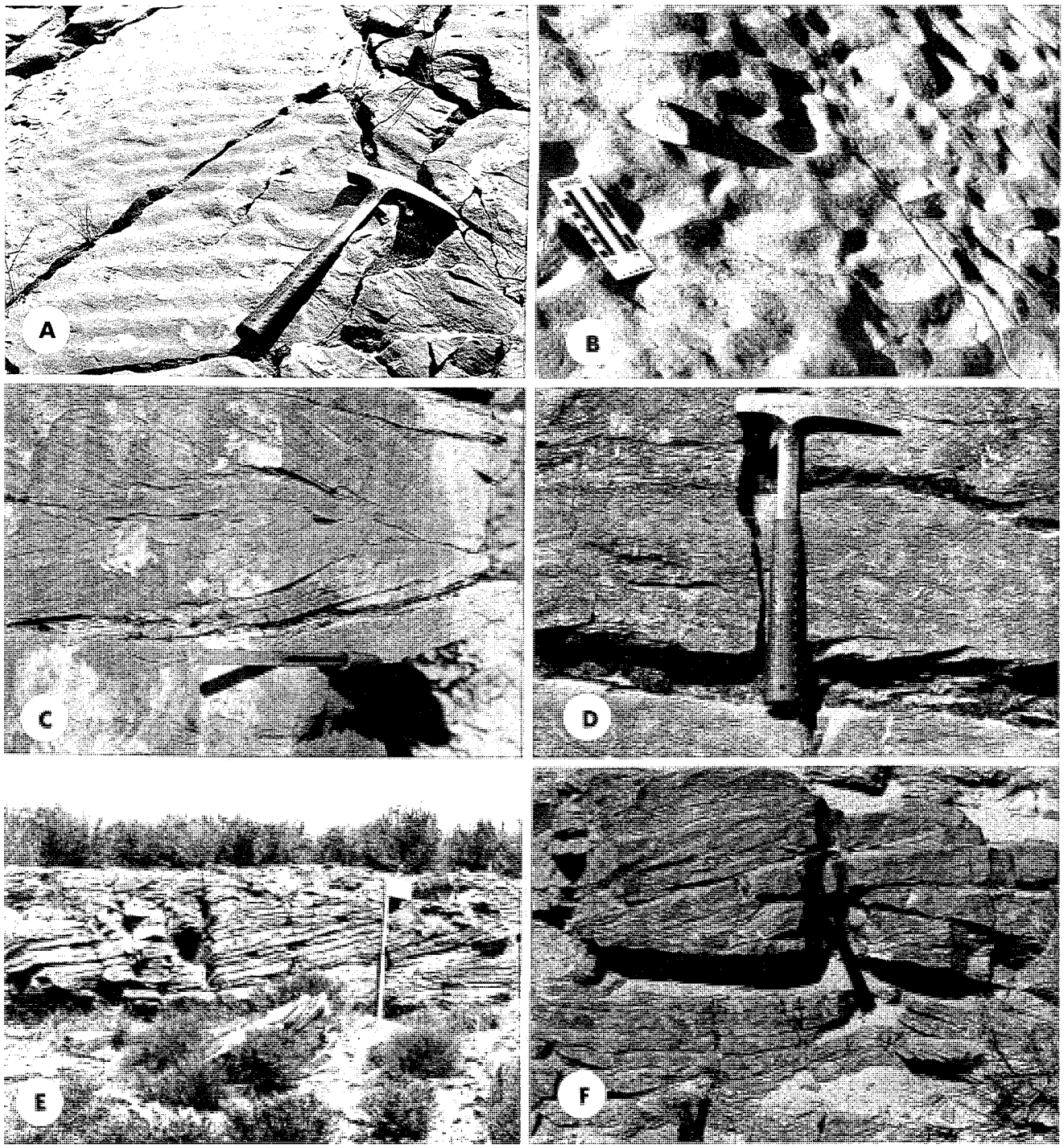

FIGURE 23.—*(A) Shallow-water wave ripple marks in oolitic grainstone, unit 51, section 5. (B) Ripple markings on underside of fallen grainstone block, unit 51, section 7. (C) Three-dimensional view of herringbone cross-bedding in oolitic grainstone, unit 51, section 7. The pen is aligned in the direction of one rock face, and normal to it is the shadow of the pen on the other rock face. (D) Wave ripple cross-bedding in oolitic grainstone, unit 51, section 5. (E) Several sets of large planar cross-bedding, unit 51, section 9. Jacob's staff for scale, 1.5 m. (F) Medium scale festoon cross-bedding in oolite grainstone, unit 51, section 5.*

FIGURE 24.—*A group of oyster colonies piled in the backyard of Milt Holt of Gunlock, Utah. Lens cap for scale. An oyster colony specimen is stored at BYU as #4011.*

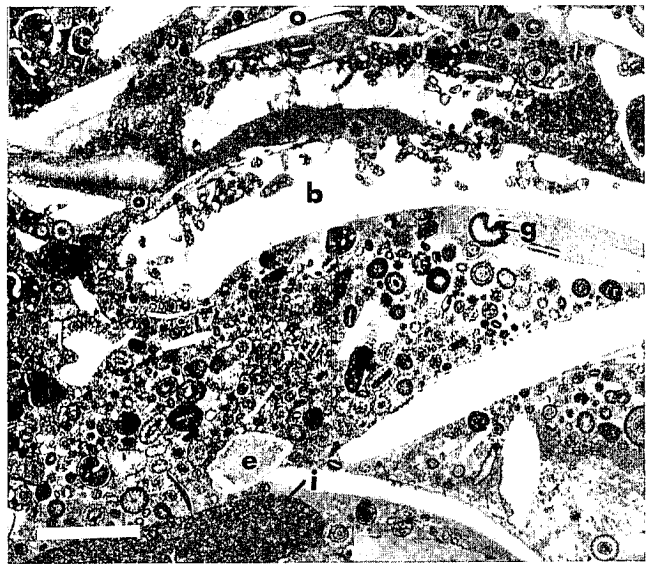

FIGURE 25.—*Photomicrograph of borings in bivalve fragments (b) of fossiliferous packstone, unit 58, section 7. Oolites, gastropods (g), echinoderm fragments (e), intraclasts (i), quartz silt, and* Ostrea *fragments (o) are cemented together in lime mudstone matrix. Bar is 2 mm long.*

FIGURE 26.—*Fossiliferous packstone, unit 56, section 10, fills channels (arrow) cut into siltstones below. Pencil for scale.*

cite cement fills pores between cryptic allochems that may be peloidal ghosts of oolites or bioclasts.

PALEONTOLOGY

Fossils were found in oolite-rich parts of members A, C, and D. Body and trace fossils were concentrated in member D. No fossils were found in members B, nor E. Only peloidal material and one recrystallized *Pentacrinus* columnal were observed in member F. Body fossils in the Carmel Formation of the study area represent a restricted molluscan fauna dominated by bivalves. Gastropods, echinoderms, coelenterates, bryozoans, foraminifers, ostracodes, and radiolarians(?) are also present. Most fossils are disarticulated and broken. Only oyster colonies in the upper part of member D and various stromatolites in members C and D grew in situ.

MOLLUSKS

Abraded and transported mollusk fragments are the predominant macrofossils in the Carmel near Gunlock. Bivalves constitute over 90% of the mollusk debris, and gastropods the remainder.

Bivalves

Bivalves occur in members A, C, and D. Densely populated layers are in semiresistant oolite-siltstone of member D immediately below the Dakota(?) Conglomerate in section 10 (fig. 7). There isolated valves of *Camptonectis platessiformis* (White), *Lima (Plagiostoma) occidentalis* Hall and Whitfield (fig. 13G), and *Ostrea (Liostrea) strigilecula* White were collected. Oyster colonies (fig. 24) of *Ostrea (Liostrea) strigilecula* White

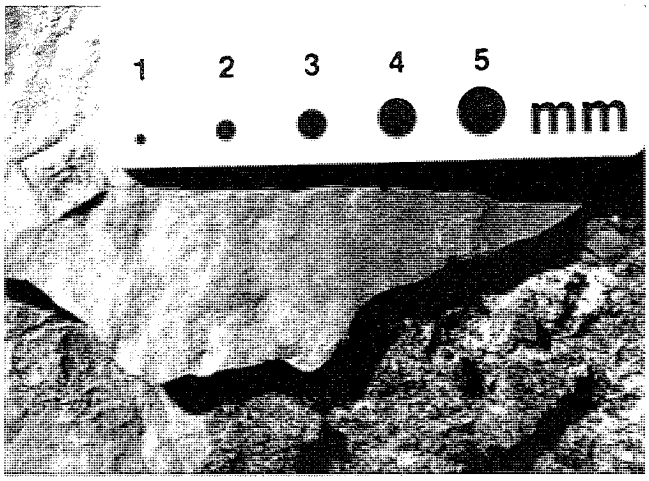

FIGURE 27.—*Halite hopper crystal molds in unit 67, section 7 (BYU #4012).*

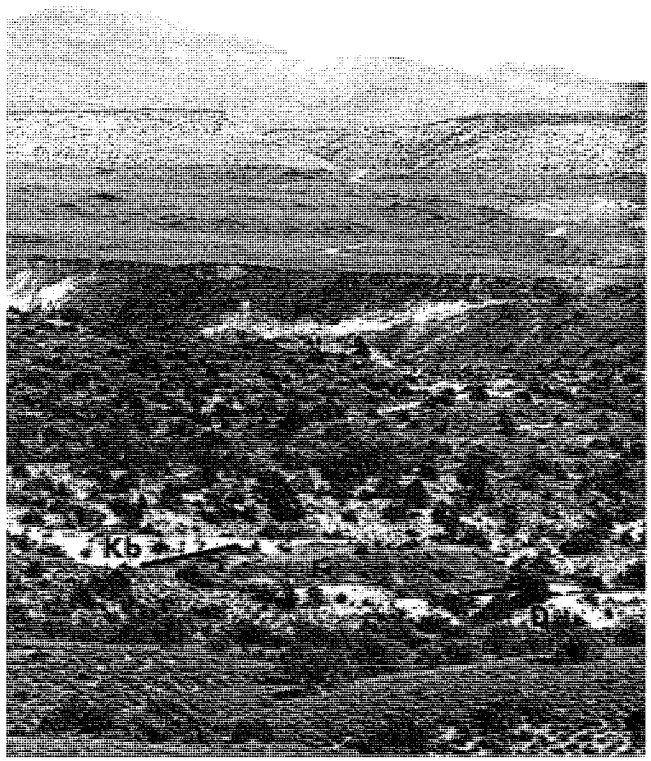

FIGURE 28.—*View east to section 4b, with Pine Valley Mountains in the background. The upper part of member D and the lower part of member E are preserved below a thin layer (3 cm) of Cretacous Dakota(?) Conglomerate and a sequence of Cretaceous bentonite (Kb) in this section.*

occur in the upper parts of member D in sections 4b, 5, 6, 7, and 8 (fig. 8). Oyster boundstone horizons have been removed from other sections by pre-Dakota(?) erosion and/or subsequent faulting.

Poorly preserved steinkerns of *Modiolus subimbricatus* (Meek) and *Pronoella* cf. *P. uintahensis* Imlay were observed on upper bedding surfaces of lime mudstone in member C. Bivalve shells replaced by silica weather out in relief on the top surface of member A. The bivalves *Gervilla* cf. *G. montanaensis* Meek, *Vaugonia conradi* (Meek and Hayden), *Astarte (Coelastarte)* cf. *(C.) livingstonensis* Imlay, and *Trigonia americana* (Meek) have been collected in the study area from the Co-op Creek Member by Imlay (1964). *Ostrea* and *Modiolus* were typically shallow-water attached forms, *Vaugonia* and *Pronoella* were bottom-dwelling forms, and *Camptonectes* was a free-swimming form (Imlay 1964).

Gastropods

The second-most abundant group of fossils in the Carmel of the study area are gastropods. They are seen in thin sections (figs. 21, 25) and often occur on the tops of oolite beds or as debris within oolite sands (fig. 13C). Gastropods are abundant in members A and D. Numerous *Cylindrobullina?* sp. were found among neritid gastropods on the top surface of member A near section 4. *Rhabdocolpus viriosus* Sohl occurs on bedding planes of oolitic units near the middle of member D. Sohl (1965) collected *Lyosoma powelli* White, *Lyosoma enoda* Sohl, and *Neritina phaseolaris* White from lower portions of the Co-op Creek Member near section 7. Sohl (1965) also identified and photographed specimens of *Globularia?* sp. and *Tylostoma?* sp., collected from the same locality.

COELENTERATES

Colonial corals, probably belonging to the genus *Astrocoenia* Milne Edwards and Haime, have been reported from several localities within the Co-op Creek Member in Garfield, Kane, and Iron Counties (Wells 1942). A similar specimen, 2 cm in diameter, was collected from among bivalve debris on the top surface of unit 32 in section 9 (fig. 13B). The coral, *Astrocoenia* Milne Edwards and Haime, occurs in Montana and Wyoming only in Bajocian-age beds (Imlay 1964).

ECHINODERMS

Crinoids

Numerous *Pentacrinus* columnals were observed in members C, D, and F (fig. 14B). These star-shaped columnals measure up to 2 mm in diameter and are found mixed within oolite-sands (fig. 13D). The species *Pentacrinus californicus, Pentacrinus asteriscus* Meek and Hayden, and *Pentacrinus whitei* Clark occur in Carmel strata throughout Utah (Clark and Twitchell 1915).

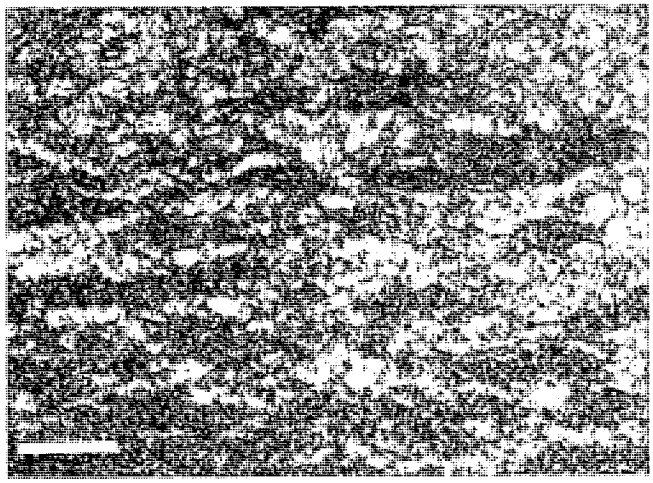

FIGURE 29.—*Photomicrograph of quartz siltstone, unit 19, section 4b. Note the large proportion of blocky calcite lenses. Bar is 2 mm long.*

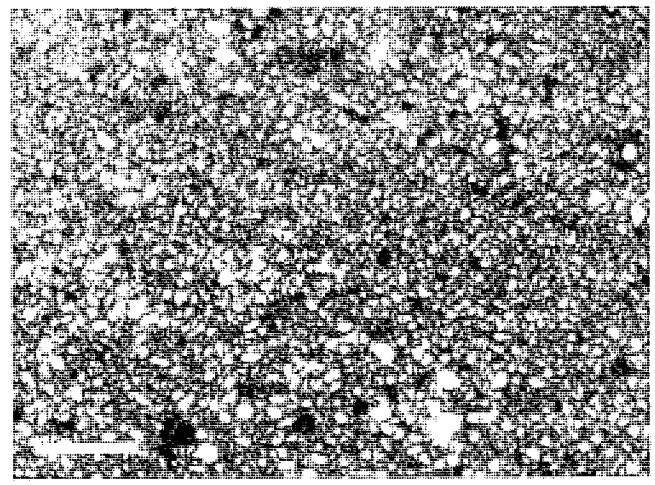

FIGURE 30.—*Photomicrograph of quartz sandstone, unit 15, section 3b. Bar is 2 mm long.*

Echinoids

Several regular echinoids were collected from unit 56 in section 10 (fig. 26). Specimens measure 12–14 mm in diameter and 4–6 mm in height (fig. 13A). The echinoids were found with bryozoan debris and large fragments of disarticulated mollusks. Echinoid spines up to 4 mm long, echinoid fragments, and disassociated echinoid plates are also preserved in many oolitic units (fig. 13C–D).

An echinoid from the lower part of the Co-op Creek Member near Carmel Junction was identified by Taylor (1981) as belonging to the genus *Diademopis* Desar. Echinoids have been found in correlative strata in northern Utah, Wyoming, and Idaho (C. W. Cook 1957; Miller 1928, 1929; and Phillips 1963).

BRYOZOANS

Sheets of cyclostome bryozoans were collected from echinoid-bearing beds described above (fig. 13E). Bryozoans were observed in most thin sections of fossiliferous packstone to grainstone (fig. 21). Bryozoans found near Mount Carmel Junction were identified as *Mesenteripora* Blainville by Taylor (1981).

MICROFOSSILS

Ostracodes, foraminifers, and radiolarians(?) were observed in thin sections of lime mudstone from members C and D (fig. 14A–D). Blakey and others (1983, p. 84) identified a Jurassic foram, *Vauginulina*, in pellet-rich lime mudstone of the Co-op Creek Member in southern Utah.

TRACE FOSSILS

Trace fossils observed in members C and D are usually visible beneath ripple-marked siltstone surfaces and on the upper surfaces of oolite grainstone beds. Trace fossils in the study area can be grouped into the *Trypanites, Skolithos,* and *Cruziana* ichnofacies (fig. 20A–D) as defined by Frey and Pemberton (1984).

Trypanites

The *Trypanites* hardground ichnofacies occurs on upper surfaces of fossiliferous packstone to wackestone in member D as several mm deep and 5-mm-diameter cylindrical to vase-shaped borings, oriented normal to the surface (fig. 20D). Some borings also penetrate *Ostrea* shells scattered on the rock surface. This suggests that some lithification of the sediments occurred prior to the excavation by boring organisms. In rare instances, small bivalves in growth position were observed in the borings (fig. 13F).

Cruziana

The *Cruziana* ichnofacies is characterized by a variety of crawling and feeding structures formed by suspension- and deposit-feeding organisms in moderate-energy, subtidal zones below fair-weather wave base but above storm wave base. These types of conditions are found in estuaries, bays, and lagoons, as well as in epeiric seas (Frey and Pemberton 1984). This ichnofacies was observed on the surfaces of sandy-oolite grainstone as well as beneath rippled oolite-siltstone beds in member D.

Three general forms of trace fossils in the *Cruziana* ichnofacies were observed in the study area. The first type occurs on the surface of sandy-oolitic grainstone and consists of 2–3 mm wide, sinuous, bilobate-ridged crawling trails with obliquely placed transverse pads (fig. 20C). The bilobate ridges are separated by a median furrow.

FIGURE 31.—*View northwestward toward section 1b with Jackson Peak in the background. Cretaceous age Dakota(?) Conglomerate (Kd) underlies Iron Springs Formation (Ki) and rests unconformably on member F of the Carmel Formation. Member E of the Carmel is hidden by trees in the valley bottom.*

The second type of trace fossil is found on the undersides of rippled siltstone beds and consists of intrastratal, unilobate feeding structures formed by an interweaving net of tube structures 1–5 mm in diameter (fig. 20A). The other trace fossil observed is a peculiarly large, 10-cm-wide crawling structure observed in sandy-oolite grainstone in upper member D, section 1a (fig. 20B).

The ichnogenus *Thallasinoides* has been reported from the Co-op Creek Member in Kane County (Voorhees 1978, p. 52).

Skolithos

The *Skolithos* ichnofacies is found in sedimentary rocks that accumulated in moderately high energy conditions, such as in shoals and spits. The ichnofacies is characterized by vertical to subvertical dwelling structures formed by suspension feeders as a result of substrate aggradation or degradation (Frey 1975). Subvertical burrows were observed in oolite-siltstone and rarely in grainstone of member D (fig. 20F). Intense reworking of shoal sediments and associated biogenic structures probably obliterated most of the *Skolithos* ichnofacies-type traces from grainstone deposits.

Subvertical burrows in oolite-siltstone were probably formed by burrow makers that were carried into lagoonal environments by storm currents. Conditions remained favorable for burrowing organisms for a period of time. However, stagnant lagoonal sedimentation eventually prevailed, preserving the burrows formed by these displaced burrowers.

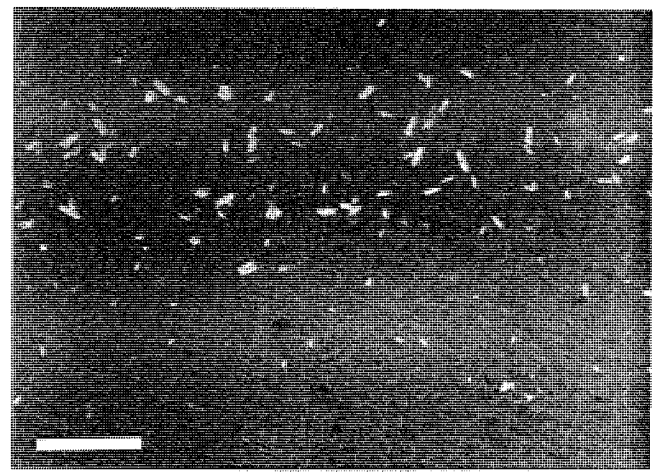

FIGURE 32.—*Photomicrograph of calcitized gypsum crystals in lime mudstone, unit 11, section 1b.*

DEPOSITIONAL ENVIRONMENTS

Low-energy sedimentary rocks in the Carmel Formation of the study area (such as lime mudstone, algal stromatolites, oyster colonies, and red beds) mixed with typical high-energy sediments and sedimentary structures such as herringbone and wave-ripple cross-bedded oolite grainstone, indicating deposition in arid, warm, shallow-marine to peritidal environments. These environments

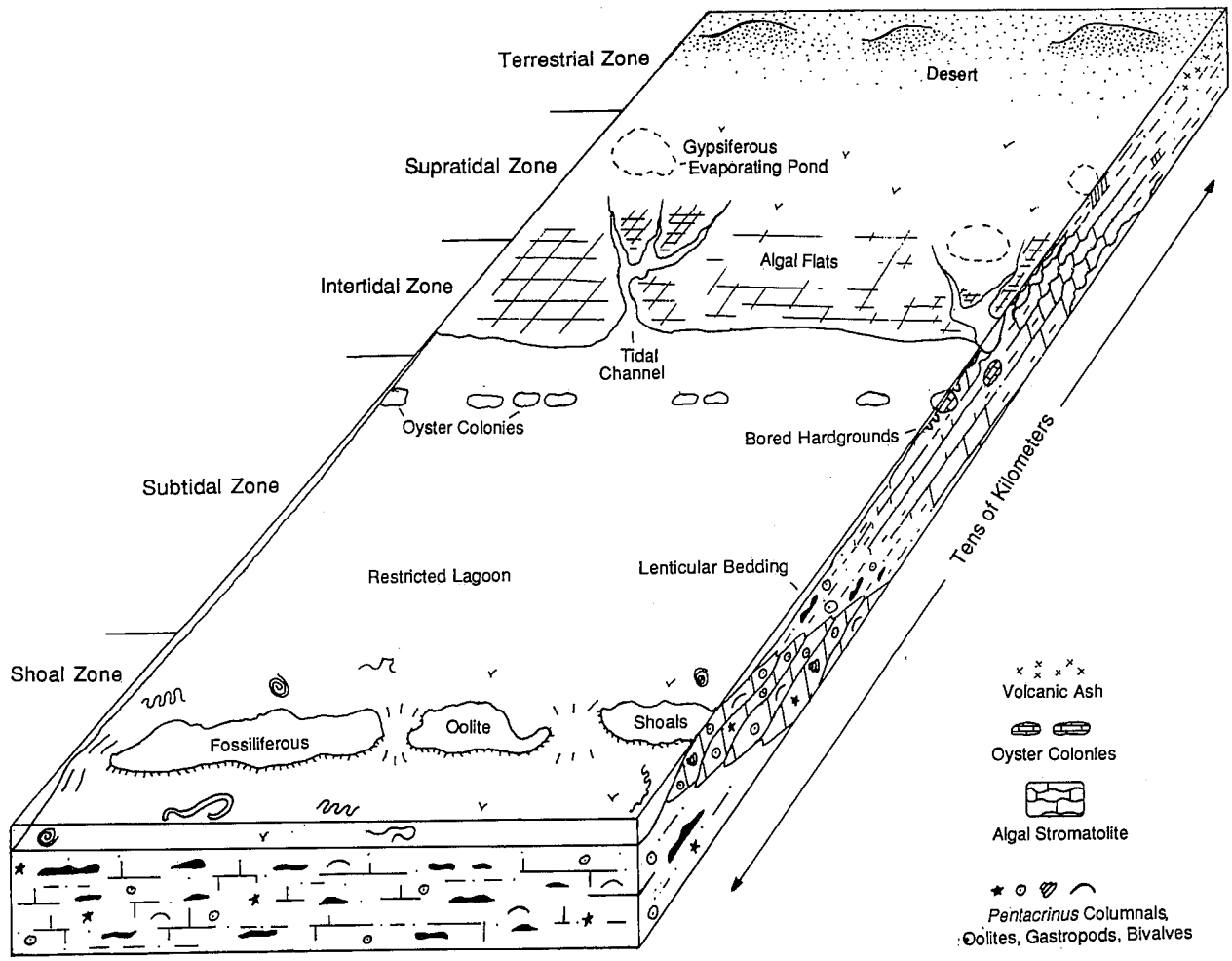

FIGURE 33.—*A schematic representation of the depositional environments in the study area during Carmel sedimentation.*

range from partially open marine or barrier shoals and sand bars to tidal flats and terrestrial conditions (fig. 33). Many similarities exist between the sedimentary record observed in the study area and that recorded by researchers (Ginsburg 1975, Hardie 1977, Heckel 1972, James 1984, Logan and others 1970, Newell and Rigby 1957, Shinn 1983) in studies of shallow-marine and tidal flat environments in modern-day coastal areas of Western Australia, the Bahamas, and in numerous ancient deposits. However, the best modern analogue for Carmel sedimentation is along the hot, arid, coastal region of the Persian Gulf. The Persian Gulf is similar to paleogeographic reconstructions of the Carmel–Twin Creek seaway in several ways (fig. 4). The Gulf area lacks an abrupt shelf margin, is isolated from direct oceanic influences, is close to the equator, and is adjacent to eolian sand seas (Purser 1973). Carmel strata of the Co-op Creek and Crystal Creek Members are replaced by eolian beds of the Page Sandstone farther east in south central Utah, and strata equivalent to the Winsor Member also contain scattered eolian sandstone lenses farther east (Blakey and others 1983).

SHOAL ZONE

Holocene deposits of oolite shoals, often referred to as bank-margin carbonate sand buildups, have been studied extensively by workers in modern shallow-marine seas near the Bahamas (Ball 1967; Halley and others 1983; Harris 1983; Hine 1977, 1983; Hine and others 1981; Illing 1954), in the Persian Gulf (Loreau and Purser 1973), and in Western Australia (Davies 1970a). Sediments and sedimentary structures indicative of shoals in the Carmel include intensely cross-bedded, sandy-oolite grainstone to packstone in members D and C. The continuity of thin intertidally deposited units over great distances (fig. 8) and the thinness of oolite grainstone to packstone bar deposits and shoals indicate that the Carmel sea in the study area was shallow and the sea-floor gradient low. Oolite grainstone units are less than 2 m thick, and shal-

low-water wave ripples occur on their bedding surfaces. Blakey and others (1983) suggest that the Carmel sea was less than 5 m deep in this area.

Shoals and bars formed barriers to currents and waves in the shallow sea and allowed low-energy lime mud and siltstone to accumulate in protected lagoons and tidal flats (fig. 33). Large foreset beds of planar cross-bedded and small- to medium-size festoon cross-bedded oolites (fig. 23E–F) in member D, probably formed on the leeward side of these shoals and bars. Planar cross-bedding develops in modern shoals as a result of sand spillover (Ball 1967), foreshore accretion in beach deposits (Inden and Moore 1983), and by longshore currents over spitlike platforms (Friedman and Sanders 1978). Small- to medium-size festoon cross-beds form in oolite sand bars (Wilson and Jordan 1983, p. 308).

Shallow-water wave ripples and herringbone cross-bedding (fig. 23A, C) occur near the top of oolite grainstones and probably formed on the mid-to-shallow landward side of shoals. These rocks lack in situ organisms and trace fossils. Sediments of the central portions of modern shoals in the Bahamas are intensely ripple marked and devoid of in situ organisms and biologically produced structures (Halley and others 1983). Most muddy oolitic sediments, formed near the shoal zone of the Carmel Sea, were carried by ebb and flood tides into lagoonal and open-marine waters over shoal surfaces and through tidal channels. These sediments were lithified as oolitic packstone and are now interbedded with lime mudstone to wackestone and siltstone (fig. 15). The presence of oolites in lagoonal rocks is typical of modern sedimentation patterns in the Persian Gulf, where bars of rippled oolites form at the mouths of tidal channels that empty into lagoons (Purser and Evans 1973, p. 279). It is in rocks composed of mixed high-energy, well-oxygenated oolite sands and low-energy lime mud that trace fossils are observed in the study area (fig. 20). Bioturbation and burrows occur seaward and landward of modern Bahamian shoals, where ooid sands are mixed with mud and other grain types (Halley and others 1983).

TIDAL FLAT SYSTEM

Sedimentation within tidal flat systems occurs in three zones: the subtidal, intertidal, and supratidal environments. Most sedimentary structures used to identify zones of deposition within tidal flat systems overlap into adjacent environments. Recognition of sedimentary structures and stratigraphic relationships common to the tidal flat facies is important for classification of tidal flat environments. Studies of modern carbonate tidal flat systems in the Bahamas (Shinn and others 1969), the Persian Gulf (Schneider 1975), and in Western Australia (Davies 1970b; Hagan and Logan 1975) provide modern-day analogues for tidal flat facies in the study area.

Subtidal

Two subtidal zones were present in the study area during Carmel deposition. They are the lagoon and tidal channel environments.

Lagoon. Lagoons are protected, low-energy, shallow-water areas often bordered seaward by shoals, barrier islands, or reefs. Landward they are bordered by intertidal to supratidal flats. The restrictive nature of lagoons results in inefficient water circulation and subsequent increases in salinity and temperature and depletion of nutrients and oxygen. A restricted fauna is expected.

Lagoonal rocks in the study area are mainly accumulations of massive yellowish gray lime mudstone and storm-induced, rippled oolitic packstone and wackestone. Lime mudstones contain small amounts of quartz silt, peloids, gastropods, miliolid foraminifers, radiolarians(?), ostracodes, and bivalves (fig. 14). Calcitized gypsum crystal casts are also preserved (fig. 32).

Siliciclastic-dominated mudstone and siltstone lagoonal rocks of member D accumulated as a precursor to the large progradational clastic wedge of terrestrial sedimentary rocks preserved in member E. Lenticular- and flaser-bedded terrigenous lagoonal sediments, like those in member D, are related to tidal rhythms of alternating currents and slackwater in modern deposits (Reineck and Singh 1980, p. 101).

Crawling and grazing trace fossils such as those associated with lenticular-bedded oolite-rich siltstone in member D (fig. 20A) are typically found in normal open-marine conditions (Wilson and Jordan 1983). Horizons of oyster colonies (fig. 24) in upper member D also suggest a period of more suitable conditions for benthic organisms. Disk-shaped colonies are near bivalve-inhabited, bored hardground surfaces formed on fossiliferous packstone (fig. 13F). Spherical oyster colonies, on the other hand, are encased in mudstone. Encrustation and radial growth of the spherical colonies may have increased their mass and caused them to sink into the soft, muddy substrate, killing the colony. Such a development may explain their small dimensions. A similar scenario has been proposed for preservation of microbioherms in the Waldron Shale of Indiana (Archer and Feldman 1986).

Further evidence for lagoonal sedimentation of these units exists in their stratigraphic relationships and paleogeographic setting, which is similar to that described for modern lagoonal deposits where low-energy sediments grade into shoal deposits in a seaward direction and into intertidal sediments in a landward direction. This vertical relationship was observed numerous times in the mea-

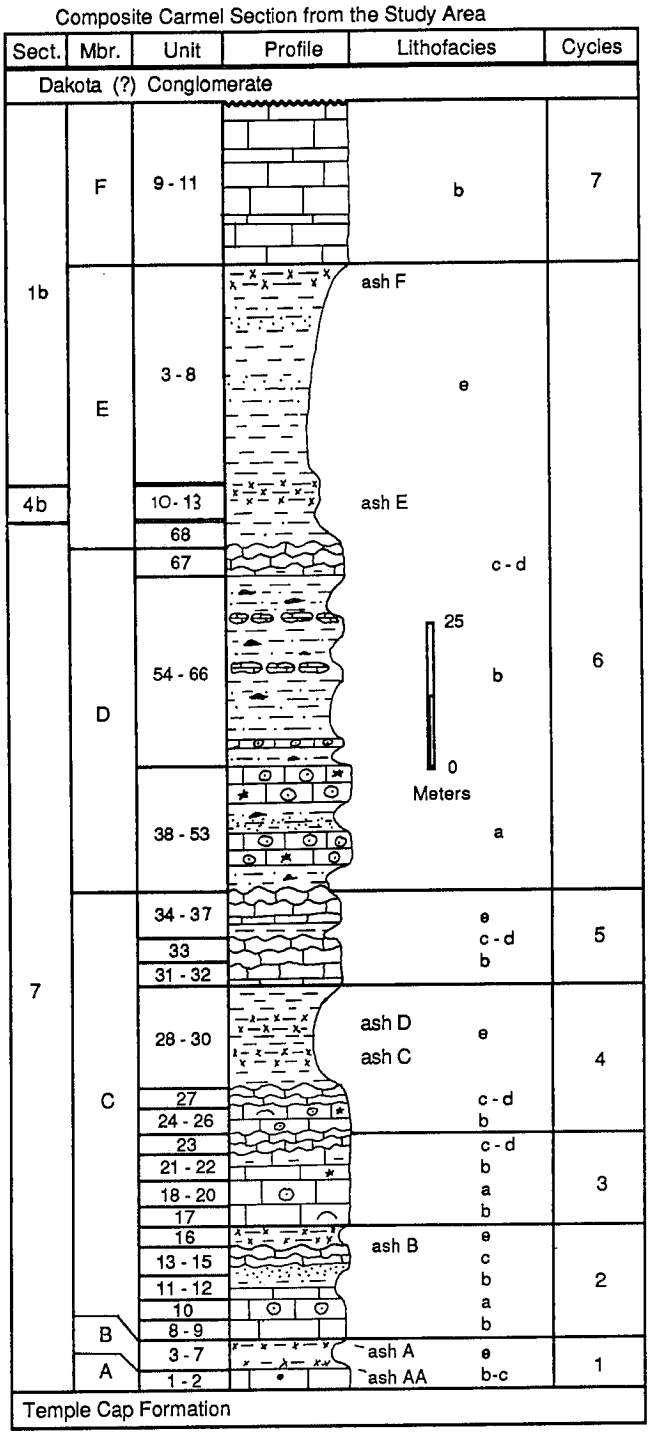

FIGURE 34.—*A complete columnar section of the Carmel Formation in the study area constructed from sections 1b, 4b, and 7 showing parameters of the seven shallowing-upward depositional cycles and their relationships to members A–F.*

sured sections (fig. 34) and is expected for typical shallowing-upward shoreline sequences (Enos 1983).

Tidal channel. Tidal channels and their tributaries are followed by tidal currents moving into and out of tidal flats. Tidal channel deposits in the study area are inferred from relict channel shapes, channel-fill bedding, and by the abundance of intraclastic debris that fills these channels. Several tidal channel units in the upper part of member D (fig. 26) show thin channel-fill bedding that conforms to relict trough-shaped channels. Tidal channels are mostly filled with coarse sand- to granule-sized lime mudstone and bioclastic intraclasts (fig. 16). The intraclasts probably originated from desiccated supratidal or intratidal flats eroded by tidal bores perhaps associated with storms.

Intertidal Flat

Sedimentary structures characteristic of intertidal flats include parting lineation, small current ripples, and algal stromatolites (fig. 17A–B). The absence of burrowing organisms suggests high environmental stress, and this, coupled with the presence of evaporites in the upper parts of algal stromatolites in members C and D, suggests that the stress was caused by extreme evaporation, such as on tidal flats in a hot, arid climate.

Intertidal environments are suggested by the presence of laterally linked hemispheroidal and columnar stromatolites (fig. 17A–B) (Logan and others 1964, Lucia 1972). Stromatolites in intermittently exposed tidal flats have been studied by Logan (1961) and Logan and others (1964) in very shallow water to intermittently emergent and hypersaline tidal flat conditions in Australia. They noted that columnar stromatolites are generally restricted to more turbulent exposed headlands while laterally linked hemispheroidal stromatolites are usually characteristic of lower-energy, protected flats and tidal ponds. Stromatolites are confined to high intertidal and low supratidal environments in the Persian Gulf (Illing and others 1965) and may indicate the same position in Carmel rocks.

The presence of evaporites in the upper part of the intertidal zone in arid climates of the Persian Gulf precludes the presence of most burrowing organisms (Shinn 1983). The existence of calcite-filled evaporite nodules (fig. 17E–F) interspersed within laminated horizons in the study area suggest similar reasons for absence of burrowing organisms in tidal flat deposits of the Carmel.

Supratidal Sabkha

The supratidal sabkha is the coastal area above normal or mean tide, submerged only during spring and storm tides. Sedimentary structures and rock types in the study area that are characteristic of supratidal sedimentation

include desiccation cracks, raindrop impressions, fenestrae, solution breccia, and evaporite structures. The presence of evaporites in sabkhas is controlled by climate (Shinn 1983). Sabkhas in the hot, arid environment of the Persian Gulf contain evaporites, but those in the more humid Bahamas do not.

Desiccation cracks occur on subaerially exposed water-saturated sediments, such as on dried-up lagoon surfaces and sabkhas. They are locally associated with raindrop imprints (fig. 17D). These features indicate subaerial exposure of sediment surfaces. Raindrop imprints in muddy sediments are preserved chiefly in areas receiving only occasional and brief rains. Thus they have been reported mainly in arid and semiarid climates (Reineck and Singh 1980). Fenestrae (fig. 17E–F) and gypsum crystals, like those in the study area, are also considered reliable indicators of supratidal deposition (Shinn 1983).

Fenestrae in rocks of the Carmel Formation generally exist as irregularly distributed, calcite-filled, bubble-shaped vugs that increase in quantity toward the top of stromatolitic units and are an indication of increases in salinity that may have finally deterred algal growth. The nodules probably represent expansion during development of supratidal gypsum rosettes. Nodules of gypsum occur as large isolated rosettes several centimeters across in modern tidal flats of the Persian Gulf and increase in abundance and size landward Shinn 1983). Chalcedony fills some of the fenestrae in the study area and is reported to be of a length-slow type in void-fillings of the Carmel east of the study area (Voorhees 1978). Length-slow chalcedony is found almost exclusively in chalcedony replacements of evaporites formed supratidally (Folk and Pittman 1971).

Halite hopper casts in member D (fig. 27) and evaporite solution breccia (fig. 18) in member C are supportive evidence for supratidal deposition in parts of the Carmel. A supratidal origin for gypsum associated with evaporite solution breccia is suggested (James 1984, Lucia 1972).

Large ripples on the upper surface of oolitic packstone in member A (fig. 11) may have formed by seiche currents moving across the supratidal zone. Studies of storm deposits on tidal flats of Florida and the Bahamas indicate that large quantities of subtidal sediments are washed onto supratidal flats during storms (Ball, Shinn, and Stockman 1963). Scarcity of erosional processes on supratidal flats tends to allow preservation of storm accumulations. Member A may have formed this way. It is a 2-m-thick, isolated, yellowish gray carbonate unit underlain and overlain by thick sequences of reddish brown siliciclastic strata deposited high in the supratidal zone. The stratigraphic location and intensely ripple-marked surface of the oolitic packstone suggest that its sediments were transported from offshore to a supratidal location by vigorous and perhaps storm-driven currents.

TERRESTRIAL

The term terrestrial is applied to environments high in the supratidal zone where sediments uninfluenced by marine processes accumulated. Deposits labeled terrestrial in this study may have accumulated in the same physiographic location as the supratidal zone. However, the change from carbonate to siliciclastic deposition indicates a distinct difference in sedimentation styles and therefore seems to warrant a separate category. The transition from supratidal carbonates to siliciclastic red beds is common in tidal flats of Permian age in west Texas and New Mexico (Dunham 1972). Modern Baja California sediments grade laterally from reduced gray silt in the intertidal zone to oxidized brown silt in the supratidal environment (Thompson 1968).

The red beds of members B and E constitute the majority of sediments in this category. Volcanic ashes in member C, grouped under terrestrial environments, may have been deposited in low-energy intertidal or perhaps lagoonal settings. They are grouped with other terrestrial environments in this report, based on stratigraphic position.

The thick sequence of red-bed mudstone, siltstone, and two thin sandstone beds in member E, as well as the thinner red-bed sequence in member B, represent terrigenous deposition during progradation of a siliciclastic wedge into the Carmel basin. Red beds of member B are separated from similar red beds in the Temple Cap Formation by member A. Temple Cap red beds were probably deposited on a broad tidal flat (Rigby 1986b). Similarly red beds in member E occur conformably over a sequence of algal stromatolites and supratidal rocks containing salt crystal casts and three thin, mottled, pale green to reddish brown zones with rootlike features.

In general, brown- to red-colored sedimentary rocks containing evaporites indicate deposition in oxidizing subaerial environments. Red beds often form by postdepositional, interstratal oxidation of iron-bearing grains to hematite in warm, arid environments (Walker 1967). The source of the iron is usually ferromagnesium minerals (Reineck and Singh 1980) such as biotite commonly found in volcanic ash beds in the study area. The presence of broad, blocky calcite lenses interpreted as caliche zones (fig. 29) in the Carmel red beds, as well as the stratigraphic position of the red beds above and below supratidal deposits, suggests that the red beds were deposited subaerially in an arid environment.

CYCLIC DEPOSITION

Sediments in the Carmel Formation near Gunlock record two major transgressions documented in Middle Jurassic rocks of the Western Interior (Imlay 1957) and at least seven secondary, shallowing-upward carbonate se-

quences. The two major transgressions correspond to global fluctuations of sea level in Middle to Late Jurassic time (Vail and others 1977, fig. 2). The global rise in sea level and formation of worldwide Jurassic cyclothems is attributed to tectonically controlled eustatic sea-level changes caused by episodic plate movements and rising oceanic spreading centers (Hallam 1975). Heller and others (1986) suggested that subsidence of the Western Interior during the Middle Jurassic probably reflected tectonic events west of and prior to the Sevier orogeny, since no coarse clastic material that came from the Sevier orogenic belt exists in the Carmel and other units of this age (Imlay 1980). They suggested that thermal subsidence following a Middle Jurassic thermal metamorphic event in northwest Nevada (Snoke and Lush 1984) or perhaps flexural subsidence as a result of thrust plate emplacement and loading in Nevada and northwest Utah (Allmendinger and others 1984) may have formed the Middle Jurassic basin in the Western Interior.

Portions of seven asymmetric shallowing-upward carbonate sequences occur in the Carmel Formation within the study area (fig. 34). One partial cycle spans members A and B, four small cycles occur in member C, one large cycle spans members D and E, and the beginning stages of a seventh cycle is in member F. These cycles represent rapid rises in sea level, or abrupt basin subsidence, followed by sedimentary progradation and fill. The cycles may reflect second-order changes in the basin caused by tectonic movement at or near the Andean-arc-type margin of western North America or perhaps minor sporadic rises in sea level. The seven volcanic ashes within the secondary cycles in the study area document that sedimentation was contemporaneous with nearby volcanic disturbances. Others have suggested that the second-order cycles in the Carmel Formation may be a result of minor epirogenetic movements or climatic changes related to Milankovitch processes or orbital variations and axis translation (Richards 1958).

An idealized shallowing-upward sequence grades vertically from an oolite shoal-zone lithofacies to a lagoonal lithofacies, followed by intertidal and supratidal lithofacies, and finally to terrestrial lithofacies (fig. 35). This model is similar to idealized models of shallowing-upward carbonates proposed by James (1984) and Wilson (1975). Third-order transgressions and regressions and incomplete sequences resulting from nondeposition are present in each cycle.

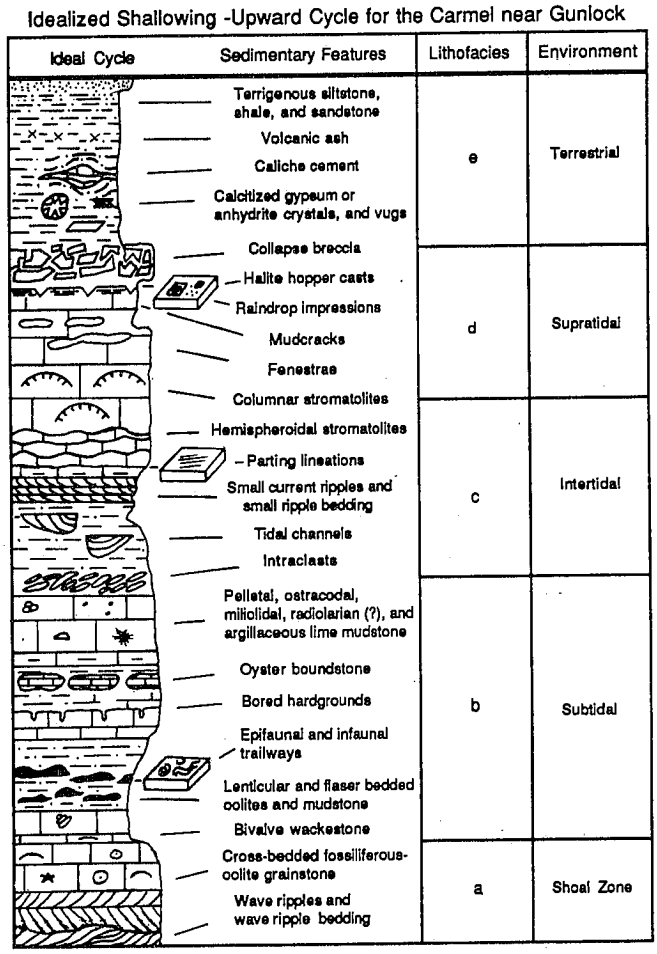

FIGURE 35.—*An idealized shallowing-upward cycle for the Carmel Formation near Gunlock showing five lithofacies (a–e) and their associated sedimentary features and environmental classification.*

GEOCHEMISTRY

Chemical analyses were performed on carbonate samples taken from sections 1 and 10. The analyses were performed to measure differences, if any, in chemical composition of carbonate lithologies between the two geographic extremes of the study area. It was postulated that chemical alteration from fluids migrating along the Gunlock fault may have enhanced dolomitization of the sediments in section 10, but the analyses do not substantiate this. However, the data does document chemical differences in units that correspond with shifts in environments of deposition vertically within sections and laterally between sections. Analyses for element enrichment (Cu, Ag, B, Fe, Sr) typically found in sabkha deposits were also performed on rocks of section 1. The results were nonconclusive (see Nielson 1988).

INSOLUBLE RESIDUES

The amount of insoluble residue in marine deposits generally is inversely proportional to the distance from shore (Trask 1937). Percentages of insoluble residue from

carbonates in this study are higher in facies deposited closer to shore, with the exception of some sandy-oolite grainstone in member D (fig. 36). Units with high proportions of insoluble residue generally contained fewer fossils than those with moderate levels.

Percentages of insoluble residue generally increase in rock type from grainstone to packstone to wackestone to lime mudstone and algal stromatolite. High percentages measured in some oolite grainstones resulted from the large amount of quartz sand and silt that served as nuclei to the oolites, as well as the abundant quartz sand and silt lenses that exist without carbonate coatings in some grainstone units in member D (fig. 22).

An eastward increase in percent insoluble residue is evident between comparison of equivalent units in sections 1 and 10. This is consistent with regional paleogeographic reconstructions showing an eastward gradation of Carmel strata into nonmarine siliciclastic deposits (Peterson 1988b, p. 71).

CALCIUM AND MAGNESIUM

Thin-section analysis of carbonates indicates that no major amount of dolomitization has occurred. Magnesium carbonate reaches a maximum in section 1 (unit 14) of less than 14% by weight, and only slightly more than twice that in section 10 (unit 29). These higher $MgCO_3$ percentages occur in algal stromatolites formed in highly evaporative supratidal zones.

Data plots illustrate an inverse relationship between Ca/Mg ratios and insoluble percentages in all rock types of the study area, except for some sandy-oolite grainstones in member D (fig. 36). Studies by Chilingar (1953, 1956, 1960, 1963) and Siegel (1961) show that Ca/Mg ratios in calcareous sediments from the Florida Keys, the Great Bahama Bank, and the Persian Gulf increase seaward and in water depth. Chilingar concluded that the Ca/Mg ratio lines parallel isothermal lines (1953, p. 207) and, hence, most likely parallel isosalinity lines also. In sulfate-rich waters, calcium first precipitates as $CaSO_4$ in gypsum. The enhanced magnesium percentage in the remaining sulfate-poor waters favors precipitation of high magnesium calcite. Most ancient sedimentary deposits with high concentrations of magnesium are associated with evaporite deposits. Units in the study area that have higher magnesium percentages (fig. 36) accumulated under more hypersaline conditions. Units that contain abundant fossil remains have lower magnesium percentages than those that contain few or no fossil remains. Magnesium concentrations are higher in section 10 than section 1. This relationship also suggests eastward shallowing toward the ancient shoreline.

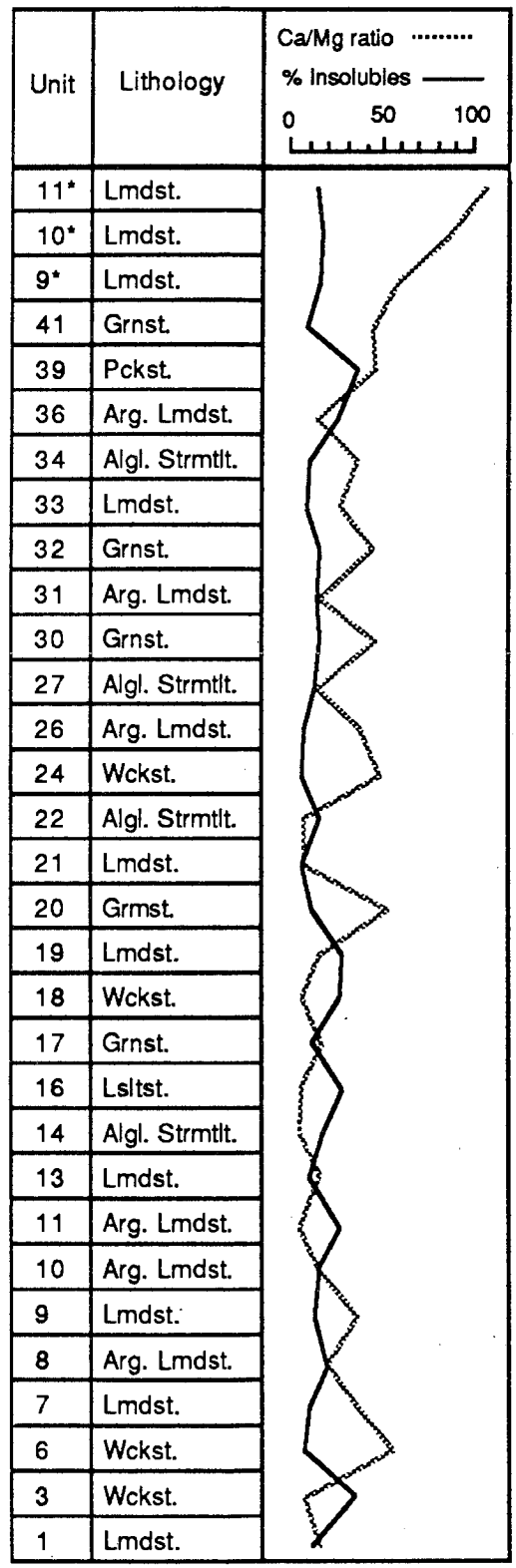

FIGURE 36.—*Plots of geochemical data from carbonates in section 1.*

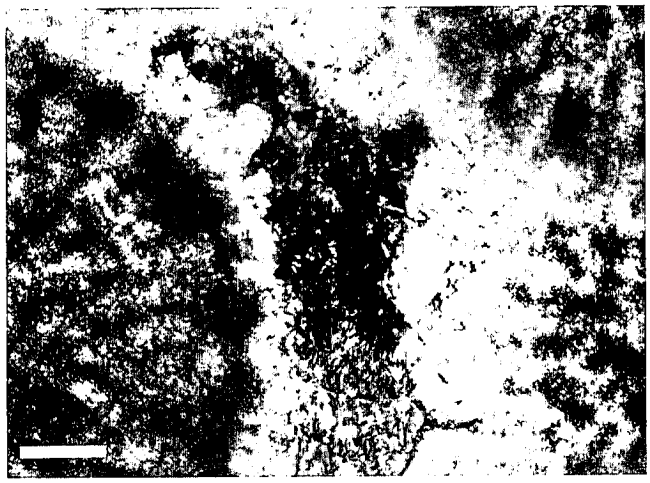

FIGURE 37.—*Photomicrograph of oolites under cross-polarized light showing isopachous stubby calcite cement, unit 52, section 7. Bar is 50 microns long.*

FIGURE 38.—*Secondary banding in recently exposed rock near the base of section 10, unit 11. Pencil or scale.*

DIAGENESIS

Diagenesis in Carmel rocks near Gunlock has done little to destroy their original microsedimentary structures, fabric, and allochemical constituents. The main diagenetic effects are evaporite dissolution, replacement crystallization, neomorphism, and minor chemical alteration. Carbonate allochems are cemented by thin isopachous layers of stubby calcite cement in grainstone rock types. Interparticle porosity is filled with coarse, sparry calcite (fig. 37). Some ooids exhibit grain interpenetration, yet generally there are no grain-to-grain contacts. In most cases a cement rim intervenes. These types of grain boundaries generally result from compaction and grain interpenetration postdating cementation (Scholle 1978, p. 207). The preservation of original allochemical morphology also suggests early cementation.

Calichification is believed to have caused the thick calcite cement layers that occur between silt layers in red beds of members E and B (fig. 29). Fluids saturated in calcite were drawn between supratidal laminations by capillary wicking. The saturated solutions precipitated calcite, which caused contemporaneous layer expansion during crystallization.

CHEMICAL ALTERATION

Both thin section and geochemical data suggest that little or no secondary dolomitization in Carmel rocks occurred. Only collapsed breccia fragments of member C (fig. 18) and the mudstone matrix of member A were dolomitic. The formation of calcium sulfate in gypsiferous beds of the upper Temple Cap Formation and in the cementing media of the collapse breccia, before dissolution, increased the magnesium ion concentration in the remaining solutions high enough for dolomite formation during or soon after deposition of the carbonate units.

Peculiar, 8-cm-diameter, black and white, calcite-rimmed voids occur in joint intersections in lime mudstone in member F. The lime mudstone units contain numerous layers of calcitized gypsum crystals (fig. 32). Calcification of these units subsequent to faulting may explain the anomalously high Ca/Mg ratios recorded in the geochemical analyses (fig. 36) of this horizon.

Carbonate units in the study area contain a distinctive yellowish gray to orangish brown rust-coloration. This coloration is attributable to individual oolites and lime mudstone matrix and clasts. Fossil fragments and sparry calcite fillings show no such coloration. The rusty color is particulary intense on hardground surfaces. Hardgrounds, here and elsewhere, commonly have a rust-colored hue produced by oxidation of ferrous iron salts impregnated on their surfaces from prolonged exposure to sea water (Scoffin 1987, p. 96). Exposed bedding surfaces of strata in the Carmel Formation near the base of section 10 have been cut recently by the Santa Clara River. Carbonate units in these stream cuts exhibit a type of secondary banding along joint surfaces where oxidized yellowish brown to orangish brown material of the outer rings contrast against light bluish gray material from the unoxidized core (fig. 38).

REPLACEMENT CRYSTALLIZATION AND NEOMORPHISM

Replacement crystallization from aragonite and gypsum to calcite, and from calcite, aragonite, and gypsum to chalcedony occurred within select fossils, oolites, voids,

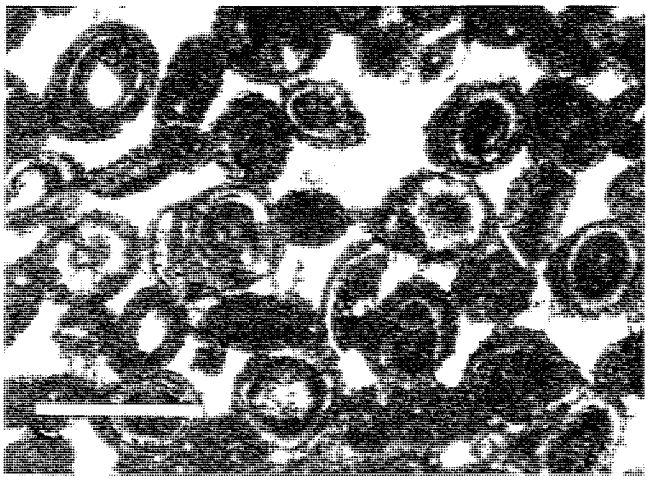

FIGURE 39.—*Partially micritized oolites, unit 30, section 1a. Bar is 0.5 mm long.*

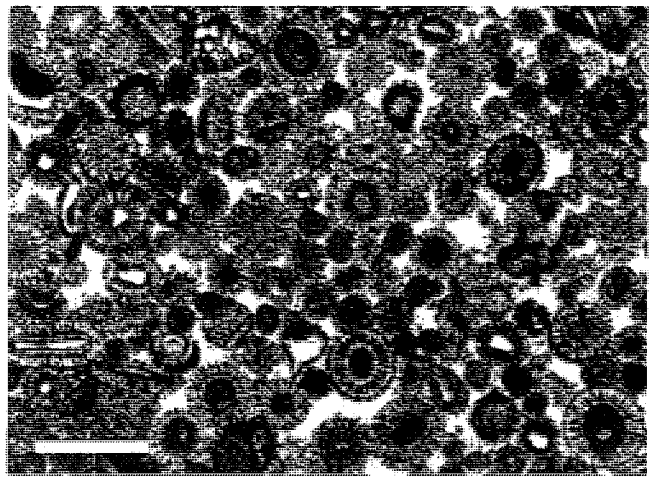

FIGURE 40.—*Photomicrograph of oolites in oolitic grainstones with concentric-radial fabric, unit 52, section 7. Bar is 0.5 mm long.*

and beds. Minor degrading neomorphism is evident in some layers where micritized oolites (fig. 39) and micritic coatings of allochemical particles occur. These beds are sandwiched between lime mudstone. The micritic envelopes may have been created by precipitation of clay-sized calcite or aragonite in abandoned microborings as those described by Bathurst (1975, p. 90) are in the Bahamas. Small-scale borings are evident in many thin sections (fig. 25).

Calcite and, on occasion, chalcedony have replaced parts of gypsum nodules in algal stromatolites (fig. 17) and parts of gypsiferous beds in evaporite solution breccia near the top of member C (fig. 18). Calcite also replaced gypsum vugs in the red-bed parts of members B and E as well some gypsum crystals that retained their crystalline form in lime mudstone beds (fig. 32) of members C and F. Length-slow chalcedony has replaced gypsum rosettes in beds of the Carmel to the east of the study area (Voorhees 1978, p. 53). Chalcedony has replaced oolites in member A (fig. 10).

Neomorphic change from aragonite to calcite is evident in all fossiliferous thin sections. Bivalve and gastropod shells show change to calcite from aragonite by either inversion or dissolution precipitation mechanisms, both of which commonly eliminate original shell microstructure (fig. 25). Fragments of originally calcitic fossils, including *Ostrea* and most echinoderm and bryozoan fragments, show little or no neomorphism or replacement crystallization. Oolites exhibit the commonly developed radial fabric found in many ancient oolite deposits (Scholle 1978, p. 118). The concentric laminations of the oolites are still visible and are cut by thin, disruptive radial crystals (fig. 40). Preservation of this concentric/radial structure has been utilized elsewhere to suggest a previous Mg calcite composition (Richter 1983, p. 112).

SUMMARY

The Carmel Formation near the town of Gunlock in Washington County, Utah, is composed of 240 m of shallow-marine to peritidal sediments that accumulated in the southern end of the narrow, restricted, Middle Jurassic Western Interior seaway (fig. 4). Carmel outcrops in the study area are the westernmost exposures of marine Jurassic rocks known in the Cordilleran region and record two major transgressions, a regression, and seven second-order shallowing-upward sequences. The study area was near 15° north paleolatitude and had a hot, arid climate during deposition. Recent low-energy sedimentation along the Trucial Coast in the Persian Gulf is a modern depositional analogue for Carmel sedimentation in the study area.

One hundred meters of Carmel strata, previously not reported to be preserved below the regionally unconformable upper contact of the Carmel in the area, is described in six informal members, labeled A–F, that include the Co-op Creek Member of Doelling and Davis (1989) and the Crystal Creek and part of the Paria River(?) Members of Thompson and Stokes (1970).

Diagenetic influences on the rock of the study area include evaporite dissolution, replacement crystallization, neomorphism, oxidation, and minor dolomitization. Geochemical analyses of the carbonate rock types document inverse relationships between insoluble residue percentages and calcium/magnesium ratios.

Seven biotite-rich volcanic ashes, up to 1 m thick, occur

interbedded in the section. Preliminary results of argon-argon and fission track studies suggest that these ashes range in age from Late Callovian to Early Oxfordian.

ACKNOWLEDGMENTS

The author extends deep appreciation to J. Keith Rigby for his encouragement and suggestions during fieldwork and preparation of this manuscript. I am also grateful to Bart J. Kowallis, Lehi F. Hintze, and Fred Peterson for reviewing the text, to Angus U. Blackham for helping with the geochemical analyses, and to Lui Huaibo from the Jianghan Petroleum Institute of China for assistance with the petrology. Members of the 1986 BYU Geology Summer Camp provided preliminary measurements and descriptions of several sections. A grant from the American Association of Petroleum Geologists and another from Brigham Young University (based on a gift from Floyd Petersen of Salt Lake City, Utah) helped defray expenses.

APPENDIX

SECTION 1B—JACKSON PEAK

Section 1b starts 700 m west and 700 m south of the northeast corner of section 10, R. 18 W, T. 40 S, in the Gunlock 7½-Minute Quadrangle at the first reddish brown siltstone that occurs below biotite-rich, pale blue green volcanic ash. This is near the base of member E just below major limestone cliffs of member F. Section 1b is separated from the continuity of section 1a by a few tens of stratigraphic meters due to faults in the valley that separate them (fig. 8, in pocket).

Unit	*Description*	*Unit Thickness (meters)*	*Cumulative Thickness (meters)*
	Dakota(?) Conglomerate: Dark brownish black to weather-stained reddish pink conglomerate.		
	Unconformity		
	Carmel Formation		
	Member F		
11	Limestone: altered lime mudstone; mottled reddish pink to yellowish gray, highly fractured, thin to thick bedded, slabby to blocky, cliff former, 8-cm-diameter vugs filled with black to white calcite crystals rare, horizontal slickensides on rock surfaces abundant, gradational.	11	84.5
10	Limestone: altered lime mudstone; pinkish gray, highly fractured, thin bedded, slabby to blocky, cliff former, gradational.	14	73.5
9	Limestone: lime mudstone; light olive gray weathers yellowish gray, thin bedded, slabby, cliff former, 5-cm-diameter calcite-filled vugs rare, one altered *Pentacrinus* columnal, gradational.	11	59.5
	Member E		
8	Mudstone: grayish yellow, thin bedded, chippy to flaggy, resistant slope former, gradational.	3.9	48.5
7	Ash F: pale olive green, thick bedded, chippy, slope former, bronze-colored biotite 1%–2%, sharp contact.	1.5	44.6
6	Siltstone: moderate reddish brown, thin bedded, slabby, ledge former, gradational.	4.1	43.1
5	Mudstone: moderate reddish brown, laminated, chippy, slope former, gradational.	6	39
4	Siltstone: moderate reddish brown, thin bedded, slabby, ledge former, gradational.	0.4	33
3	Mudstone: moderate reddish brown, interbedded with siltstone, poorly exposed in several hills and dip slopes, laminated, chippy, slope former, sharp contact.	30.6	32.6
2	Ash E: pale blue green, 2-mm-diameter black biotite 10%, thick bedded, ledgy slope former, sharp contact, correlates with unit 13, section 4b.	1	2
1	Mudstone: moderate reddish brown, laminated, chippy, slope former.	1	1

SECTION 4B—MANGANESE WASH

Section 4b starts 60 m east and 180 m north of the southwest corner of section 19, T. 40 S, R. 17 W, in the Gunlock Quadrangle at the first limestone ledge in grayish green slopes exposed below red beds of member E. This is northwest of the dirt road in Limekiln Wash. Section 4b is separated from the continuity of section 4a by a few tens of stratigraphic meters as a result of faults in the valley that separate them.

Unit	*Description*	*Unit Thickness (meters)*	*Cumulative Thickness (meters)*
	Cretaceous Bentonite		
	Dakota (?) Conglomerate	0.3	
	Unconformity		

Carmel Formation
Member E

22	Mudstone: dusky red, thin bedded, soily, slope former, thin pale green horizon near the top, sharp contact.	3	35.5
21	Mudstone: moderate yellowish red, interbedded with pale olive green mudstone, thin bedded, soily, slope former, occasional biotite, gradational.	0.2	32.5
20	Mudstone: moderate yellowish red, thin bedded, soily, slope former, gradational.	1.5	32.3
19	Siltstone: moderate reddish brown, thin bedded, slabby, calcitized gypsum vugs, ledge former, gradational.	0.1	30.8
18	Mudstone: moderate yellowish red, thin bedded, soily, slope former, gradational.	2.1	30.7
17	Siltstone: moderate reddish brown, thin bedded, slabby, calcitized gypsum vugs, ledge former, gradational.	0.2	28.6
16	Mudstone: dusky red to moderate red, thin bedded, soily, slope former, sharp contact.	4.3	28.4
15	Mudstone: mottled dusky red and pale green, possibly root perturbations, thin bedded, soily, slope former, sharp contact.	0.3	24.1
14	Mudstone: dusky red to moderate red, thin bedded, soily, slope former, sharp contact.	5.5	23.8
13	Ash E: pale blue green, abundant biotite up to 10%, ledgy slope former, correlates with unit 2, section 1b.	1	18.3
12	Mudstone: dusky red, indiscriminate bedding, soily, slope former, sharp contact.	1.8	17.3
11	Siltstone: grayish yellow, thin bedded, flaggy, slope former, gradational.	.3	15.5
10	Mudstone: dusky red, indiscriminate bedding, soily, slope former, sharp contact.	1.5	15.2

Member D

9	Limestone: algal stromatolite; yellowish gray, wavy laminated, shaly, ledge former, gradational.	1.8	13.7
8	Dip slope: yellowish gray argillaceous lime mudstone, thin bedded, slope former, gradational.	3	11.9
7	Limestone: argillaceous lime mudstone; yellowish gray, laminated, shaly, stromatolitic? resistant ledgy slope former, gradational.	2	8.9
6	Mudstone: yellowish gray, laminated, chippy, slope former, gradational.	2.2	6.9
5	Mudstone: yellowish gray, laminated, chippy, slope former.	0.1	4.7
4	Mudstone: yellowish gray, laminated, soily to chippy, slope former, sharp contact.	3.4	4.6
3	Limestone: oolitic packstone; light olive gray weathers moderate yellow, thin bedded, slabby, ledge former, 1 by 2 cm flat oyster colonies, sharp contact.	0.2	1.2
2	Mudstone: yellowish gray and orangish yellow gray, laminated, chippy, slope former, sharp contact.	0.8	1.0
1	Limestone: silty packstone; light olive gray weathers orange gray, thin bedded, slabby, oolites, ledge former, symmetrically rippled upper surface of wavelength 10 cm and wave height 1 cm indicates 150° and 330° azimuths of sediment transport, small 6-by–8-cm-diameter oblong oyster colonies, *Cruziana* ichnofacies, correlates with unit 58, section 7.	0.2	0.2

Quaternary colluvium

SECTION 7—RESERVOIR

Section 7 starts 550 m west and 850 m south of the northeast corner of section 32, T. 40 S, R. 17 W, in the Gunlock Quadrangle at the lowest limestone ledge above reddish brown siltstone of the Temple Cap Formation. This is adjacent to Gunlock Reservoir.

Unit	*Description*	*Unit Thickness (meters)*	*Cumulative Thickness (meters)*
	Dakota (?) Conglomerate: conglomerate, dark brownish black, very thick bedded, cliff former, sharp contact.		

Unconformity

Carmel Formation
Member E

68	Covered: exposed slope toward the east shows moderate reddish brown mudstone and siltstone.	3	144.9

Member D

67	Limestone: argillaceous lime mudstone; yellowish gray, lami-	1.6	141.9

	nated, shaly, ledge former, mudcracks and calcitized gypsum nodules common, halite hoppers rare, gradational.		
66	Mudstone: yellowish gray, laminated, chippy, slope former, gradational.	2.8	140.3
65	Siltstone: light olive gray, lenticular bedded with thin rippled lenses of oolites, flaky, ledgy slope former, gradational.	2.1	137.5
64	Mudstone: light olive gray, laminated, chippy, slope former, sharp contact.	2.1	135.5
63	Limestone: oyster boundstone; pale yellowish brown, thin bedded, weathers into 7-cm-diameter spherical oyster masses, encrusting oyster shells are 0.5 cm wide and 0.5 cm long, ledge former, gradational.	0.1	133.3
62	Limestone: fossiliferous packstone; yellowish gray, thin bedded, slabby, ledge former, high-spired gastropods common, bivalve fragments abundant, sharp contact.	0.4	133.2
61	Mudstone: yellowish gray, laminated, chippy, slope former, sharp contact.	7.5	132.8
60	Limestone: oyster boundstone; pale yellowish brown, thin bedded, weathers into 15 cm to 20 cm diameter, subspherical oyster masses, encrusting oysters shells are 2.5 cm long and 1.5 cm wide, ledge former. A 10-cm-thick horizon of fossiliferous packstone containing high-spired gastropods forms a thin substrate for the oyster colonies, sharp contact.	0.4	125.3
59	Mudstone: yellowish gray, laminated, chippy, slope former, sharp contact.	2.6	124.9
58	Limestone: oyster boundstone; pale yellowish brown, thin bedded, weathers into 15 cm to 20 cm diameter, subspherical oyster masses, encrusting oyster shells are 2.5 cm long and 1.5 cm wide, ledge former. A 10-cm-thick horizon of fossiliferous packstone containing high-spired gastropods forms a thin substrate for the oyster colonies, sharp contact, correlates with unit 1, section 4b.	0.4	122.3
57	Siltstone: light olive gray, lenticular bedded with thin-rippled lenses of oolites, flaky, slope former, *Skolithos* ichnofacies, gradational.	9.4	121.9
56	Siltstone: pale yellowish orange, shaly, slope former, interbedded with several 5–10-cm-thick beds of oolitic grainstone, light olive gray, shaly, ledgy, bivalve fragments and *Pentacrinus* columnals common, *Skolithos* ichnofacies, 3–4-cm-diameter oyster masses on bedding planes rare, cross-bedding indicates 20° and 200° azimuths of sediment transport, gradational.	3.2	112.5
55	Limestone: oolitic grainstone; yellowish gray, thin bedded, flaggy, ledge former, bivalve fragments common, *Pentacrinus* columnals rare, gradational.	0.9	109.3
54	Siltstone: pale yellowish orange, laminated, shaly, slope former, interbedded with several 5–10-cm-thick light olive gray oolitic grainstones, shaly, ledgy, high-spired gastropods rare, bivalve fragments and *Pentacrinus* columnals common, *Cruziana* ichnofacies, cross-bedding indicates 20° and 200° azimuths of sediment transport, gradational.	5.2	108.4
	Top of Carmel Cuesta		
53	Limestone: oolitic grainstone; yellowish gray, weathers pale yellowish orange, thin bedded, slabby, ledge former, bivalve fragments and *Pentacrinus* columnals common, *Cruziana* ichnofacies, cross-bedding indicates 170° and 350° azimuths of sediment transport, one 50-cm-thick planar cross-bed indicates a 330° azimuth of sediment transport, several 3–7-mm-thick mudstone layers divide the grainstone into slabs, forms the foundation of a dip slope.	0.8	103.2
52	Limestone: oolitic grainstone; yellowish gray weathers pale yellowish orange, interbedded with light olive gray mudstone, thin bedded, chippy, ledge former, gradational.	1.1	102.4
51	Limestone: oolitic grainstone; yellowish gray, weathers pale yellowish orange, thick bedded, slabby, ledge former, bivalve fragments and *Pentacrinus* columnals common, *Cruziana* ichnofacies, cross-bedding indicates 20° and 200° azimuths of sediment transport, several 3–7-mm-thick mudstone beds divide the grainstone into slabs, gradational.	2.5	101.3
50	Limestone: oolitic grainstone; yellowish gray, weathers pale yellowish orange, interbedded with light olive gray mudstone, thin bedded, chippy, ledge former, gradational.	1.5	98.8

49	Limestone: oolitic grainstone; yellowish gray, weathers pale yellowish orange, thin bedded, slabby, ledge former, bivalve fragments and *Pentacrinus* columnals common, *Cruziana* ichnofacies, cross-bedding indicates 20° and 200° azimuths of sediment transport, gradational.	1.7	97.3
48	Siltstone: light olive gray with yellowish bands, lenticular bedded with 40% pale orange oolite grainstone lenses, shaly to flaggy, slope former, gradational.	0.9	95.6
47	Limestone: oolitic grainstone; yellowish gray, weathers pale yellowish orange, thin bedded, slabby, ledge former, bivalve fragments and *Pentacrinus* columnals common, high-spired gastropods rare, *Skolithos* and *Cruziana* ichnofacies, cross-bedding indicates 0° and 135° azimuths of sediment transport, asymmetrical ripples indicate a 50° azimuth of sediment transport, gradational.	0.6	94.7
46	Sandstone: fine grained; yellowish gray, thick bedded, slabby, ledge former, gradational.	0.6	94.1
45	Siltstone: yellowish gray, weathers pale orange, lenticular bedded with lenses of oolitic grainstones, platy, slope former, *Cruziana* ichnofacies, gradational.	3.0	93.5
44	Limestone: oolitic grainstone; yellowish gray, weathers pale yellowish orange, thin bedded, slabby, ledge former, bivalve fragments and *Pentacrinus* columnals common, *Cruziana* ichnofacies, cross-bedding indicates 20° and 200° azimuths of sediment transport, gradational.	1.3	90.5
43	Siltstone: yellowish gray, weathers pale orange, lenticular bedded with lenses of oolitic grainstone, platy, slope former, *Cruziana* ichnofacies, gradational.	2.3	89.2
42	Limestone: oolitic grainstone; yellowish gray, weathers pale yellowish orange, thin bedded, slabby, ledge former, ripple marks and cross-beds indicate 20° and 200° azimuths of sediment transport, *Pentacrinus* columnals and bivalve fragments common, gradational.	0.6	86.9
41	Limestone: sandy-oolitic grainstone; pale greenish yellow, thin bedded, flaggy, ledge former, *Cruziana* ichnofacies, gradational.	0.5	86.3
40	Mudstone, ashy: olive green, laminated, chippy, slope former, sharp contact.	2.7	85.8
39	Limestone: sandy-oolitic grainstone; yellowish gray, weathers moderate reddish brown, thin bedded, flaggy, ledge former, biotite grains on bedding planes rare, cross-bedding indicates 10° and 190° azimuths of sediment transport, sharp contact.	0.2	83.1
38	Mudstone: olive green, very thin bedded, chippy becoming shaly upward, slope former, biotite on bedding planes common, gradational.	6.7	82.9
	Member C		
37	Limestone: argillaceous lime mudstone; yellowish gray, shaly, ledge former, stromatolitic?, gradational.	0.8	76.2
36	Mudstone: yellowish gray, laminated, shaly, slope former, capped with a 0.5-cm-thick crust of calcitized gypsum nodules, gradational.	2.6	75.4
35	Limestone: argillaceous lime mudstone; yellowish gray, laminated, shaly, slope former, capped with a 0.5-cm-thick crust of calcitized gypsum nodules, gradational.	3.1	72.8
34	Mudstone: dusky yellow, ashy, laminated, chippy, slope former, sharp contact.	1.2	69.7
33	Limestone: algal stromatolite; light olive gray, wavy laminated, shaly, calcitized gypsum nodules appear midway up the unit and increase in quantity upward to 20% at the top, ledge former, gradational.	2.1	68.5
32	Limestone: argillaceous lime mudstone; light olive gray, weathers yellowish gray, thin bedded, pencilly to blocky, fractures conchoidally, resistant slope former, gradational.	0.8	66.4
31	Limestone: lime mudstone; light olive gray weathers yellowish gray, thin bedded, pencilly to blocky, fractures conchoidally, ledge former, sharp contact.	3.4	65.6
30	Mudstone: mostly covered; yellowish gray, interbedded with pale olive green ash, laminated, chippy, slope former, biotite on bedding planes rare, gradational. Part of this unit is equivalent to ash D.	10.2	62.2
29	Ash C: grayish olive, thick bedded, chippy, slope former, black biotite 5%, sharp contact.	2.2	52
28	Mudstone: yellowish gray, weathers pale orange, laminated, shaly,	2.7	49.8

	slope former, capped with 5-cm-thick pale orange evaporite-solution breccia, sharp contact.		
27	Limestone: algal stromatolite; light olive gray, wavy laminated, shaly, ledge former, gradational.	0.8	47.1
26	Limestone: argillaceous lime mudstone; light olive gray weathers yellowish gray, thick bedded, pencilly, resistant slope former, gradational.	2.4	46.3
25	Limestone: lime mudstone; light olive gray, weathers yellowish gray, thick bedded, blocky to pencilly upward, ledge former, sharp contact.	2.9	43.9
24	Limestone: fossiliferous-intraclastic packstone; light olive gray, thick bedded, slabby, ledge former, bivalve fragments and *Pentacrinus* columnals common, unit thins in 150° and 330° azimuths, sharp contact.	1	41
23	Limestone: algal stromatolite; yellowish gray, wavy laminated, shaly, ledge former, gradational.	0.4	40
22	Limestone: argillaceous lime mudstone; yellowish gray, thin bedded, flaggy, slope former, gradational.	2.2	39.6
21	Limestone: fossiliferous wackestone; light olive gray, thick bedded, slabby and pencilly, ledge former, crinoidal debris, fractures conchoidally, gradational.	3	37.4
20	Limestone: fossiliferous packstone; pale yellowish orange, thin bedded, slabby, ledge former, *Pentacrinus* columnals common, gradational.	0.6	34.4
19	Limestone: wackestone; yellowish gray, thick bedded, chippy, interbedded with packstone, blocky, ledgy slope, biotite on bedding planes rare, gradational.	4.2	33.8
18	Limestone: oolitic grainstone; grayish yellow, thin bedded, slabby, ledge former, gradational contact.	0.6	29.6
17	Limestone: argillaceous lime mudstone; yellowish gray, thin bedded, slabby, ledgy slope former, gradational.	1.2	29
16	Ash B: grayish green, laminated, chippy, slope former, black biotite 10%, sharp contact.	1.0	27.8
15	Limestone: algal stromatolite; yellowish gray, wavy laminated, shaly, ledge former, calcitized gypsum nodules 1–2 cm in diameter increase in quantity upward to 50%, gradational.	1.7	26.8
14	Siltstone: yellowish gray, laminated, chippy, slope former, interbedded with 20-cm-thick, grayish orange, ledge-forming, oolitic grainstone, unit thickens and thins in 140° and 320° azimuths, gradational.	1	25.1
13	Sandstone: fine grained, grayish yellow, thick bedded, blocky, ledge former, weathers spheroidally, four bivalve-fragment-rich beds 2 mm thick occur 2 m up, biotite on bedding planes rare, gradational.	3	24.1
12	Siltstone: yellowish gray, very thin bedded, shaly, ledgy slope former, gradational.	2.6	21.1
11	Limestone: argillaceous lime mudstone; yellowish gray, thick bedded, chippy to pencilly, resistant slope former, 5 cm thick oolitic grainstone bed midway up, gradational.	3.2	18.5
10	Limestone: oolitic grainstone; yellowish gray to dusky yellow, thin bedded, flaggy, ledge former, cross-bedding and rippled surface indicate 20° and 200° azimuths of sediment transport, sharp contact.	0.2	15.3
9	Limestone: argillaceous lime mudstone; yellowish gray, thick bedded, pencilly to slabby, ledgy slope former, gradational.	1.9	15.1
8	Limestone: pelletal lime mudstone; light olive gray, thin bedded, blocky, ledge former, friable, bivalves rare, sharp contact.	1.5	13.2
	Member B		
7	Siltstone: moderate yellow, very thin bedded, chippy, slope former, gradational.	0.5	11.7
6	Ash A: pale green, reworked, thick bedded, chippy, black biotite 10%, slope former, sharp contact.	2.5	11.2
5	Mudstone: dark reddish brown, very thin bedded, chippy, slope former, gradational.	2.3	8.7
4	Siltstone: yellowish gray, thin bedded, flaggy, ledgy slope former, biotite grains on bedding planes rare, gradational.	1.8	6.4
3	Mudstone: bentonitic; dusky yellow, thin bedded, chippy, slope former, biotite grains on bedding planes rare, sharp contact. Partially equivalent to ash AA.	2.5	4.6
	Member A		
2	Limestone: sandy-oolitic packstone; white, weathers yellowish white, thin bedded, blocky, vuggy	1.2	2.1

	porosity 10%, cross-beds 10–30 cm wide by 2–25 cm thick, shallow-water ripples indicate 170° and 350° azimuths of sediment transport, biotite on bedding planes common, gradational.		
1	Limestone: dolomitic lime mudstone; moderate yellow, thin bedded, flaggy, ledge former, gradational.	0.9	0.9

Temple Cap Formation: interbedded dark to medium reddish brown siltstone and mudstone with occasional horizons of pale green volcanic ash, slope former.

REFERENCES CITED

Aitken, J. D., 1967, Classification and environmental significance of cryptalgal limestones and dolomites, with illustration from the Cambrian and Ordovician of southwestern Alberta: Journal of Sedimentary Petrology, v. 37, p. 1163–78.

Allmendinger, R. W., and Jordan, T. E., 1981, Mesozoic evolution, hinterland of the Sevier orogenic belt: Geology, v. 9, p. 308–13.

Allmendinger, R. W., Miller, D. M., and Jordan, T. E., 1984, Known and inferred Mesozoic deformation in the hinterland of the Sevier belt, northwest Utah: Utah Geological Association Publication 13, p. 21–34.

Archer, A. W., and Feldman, W. R., 1986, Microbioherms of the Waldron Shale (Silurian, Indiana): Implications for organic framework in Silurian reefs of the Great Lakes area: Palaios, v. 1, p. 133–40.

Armstrong, R. L., and Suppe, J., 1973, Potassium-argon geochemistry of Mesozoic igneous rocks in Nevada, Utah, and southern California: Geological Society of America Bulletin, v. 84, p. 1375–92.

Averitt, P., 1962, Geology and coal resources of the Cedar Mountain Quadrangle, Iron County, Utah: U.S. Geological Survey Professional Paper 389, 72p.

Bagshaw, L. H., 1977, Paleoecology of the lower Carmel Formation of the San Rafael Swell, Emery County, Utah: Brigham Young University Geology Studies, v. 24, p. 51–62.

Baker, A. A., Dane, C. H., and Reeside, J. B. Jr., 1936, Correlation of the Jurassic formations of parts of Utah, Arizona, New Mexico, and Colorado: U.S. Geological Survey Professional Paper 183, 66p.

Ball, M. M., 1967, Carbonate sand bodies of Florida and the Bahamas: Journal of Sedimentary Petrology, v. 37, p. 556–91.

Ball, M. M., Shinn, E. A., and Stockman, K. W., 1963, Geologic record of hurricanes: American Association of Petroleum Geologists Bulletin, v. 47, p. 349.

Bathurst, R. G. C., 1975, Carbonate sediments and their diagenesis: Developments in Sedimentology 12 (2d ed.): Elsevier Scientific Publishing Co., Amsterdam-Oxford-New York, 658p.

Blakey, R. C., Peterson, F., Caputo, M. V., Geesaman, R. C., and Voorhees, B. J., 1983, Paleogeography of Middle Jurassic continental, shoreline, and shallow-marine sedimentation, southern Utah: In Reynolds, M. W., and Dolly E. D. (eds.), Mesozoic paleogeography of west central United States: Society of Economic Paleontologists and Mineralogists, Rocky Mountain Section, p. 77–100.

Bordine, B. W., 1965, Paleoecologic implications of strontium, calcium, and magnesium in Jurassic rocks near Thistle, Utah: Brigham Young University Geology Studies, v. 12, p. 91–120.

Bullock, L. R., 1965, Paleoecology of the Twin Creek Limestone in the Thistle, Utah area: Brigham Young University Geology Studies, v. 12, p. 121–47.

Caputo, M. V., 1980, Depositional history of Middle Jurassic clastic shoreline sequences in southwestern Utah: Unpublished master's thesis, Northern Arizona University, Flagstaff, 203p.

Cashion, W. B., 1967, Carmel Formation of the Zion Park region, southwestern Utah—a review: U.S. Geological Survey Bulletin 1244-J, p. 5–9.

Chapman, M. G., 1986, Digital age and location maps of plutons in Arizona, Nevada, and Utah: Geological Society of America Abstracts with Programs, Rocky Mountain Section, v. 18, p. 345.

———, 1987, Depositional and compositional aspects of volcanogenic clasts in the upper member of the Carmel Formation, southern Utah: Unpublished master's thesis, Northern Arizona University, Flagstaff, 93p.

Chilingar, G. V., 1953, Use of Ca/Mg ratio in limestones as a geologic tool: Compass, v. 30, p. 202–9.

———, 1956, Use of Ca/Mg ratio of limestone and dolomites as a geologic tool: unpublished Ph.D. dissertation, University of Southern California, Los Angeles, 140p.

———, 1960, Ca/Mg ratio of calcareous sediments as a function of depth and distance from shore: Compass, v. 37, p. 182–86.

———, 1963, Ca/Mg and Sr/Ca ratios of calcareous sediments as a function of depth and distance from shore: Journal of Sedimentary Petrology, v. 33, p. 236.

Clark, W. B., and Twitchell, M. W., 1915, The Mesozoic and Cenozoic Echinodermata of the United States: U.S. Geological Survey Monograph 54, p. 1–341.

Cook, C. W., 1957, A new Jurassic stomechinus from the Big Horn Basin, Wyoming: Journal of Paleontology, v. 21, p. 473–75.

Cook, E. F., 1957, Geology of the Pine Valley Mountains, Utah: Utah Geological and Mineralogical Survey Bulletin 58, 111p.

———, 1960, Geologic atlas of Utah, Washington County: Utah Geological and Mineralogical Survey Bulletin 70, 119p.

Cross, W., and Howe, E., 1905, Red beds of southwestern Colorado and their correlation: Geological Society of America Bulletin, v. 16, p. 447–98.

Davies, G. R., 1970a, Carbonate bank sedimentation, eastern Shark Bay, Western Australia: In Logan, B. W., Davies, G. R., Read, J. F., and Cebulski, D. (eds.), Carbonate sediments and environments, Shark Bay, Western Australia: American Association of Petroleum Geologists Memoir 13, p. 85–168.

———, 1970b, Algal-laminated sediments, Western Australia: In Logan, B. W., Davies, G. R., Read, J. F., and Cebulski, D. (eds.), Carbonate sediments and environments, Shark Bay, Western Australia: American Association of Petroleum Geologists Memoir 13, p. 169–205.

Dickinson, W. R., 1977, Sedimentary basins developed during evolution of Mesozoic-Cenozoic arc-trench system in western North America: Canadian Journal of Earth Science, v. 13, p. 1268–87.

———, 1981, Plate tectonic evolution of the southern Cordillera: In Dickinson, W. R., and Payne, W. D. (eds.), Relations of tectonics to ore deposits in the southern Cordillera: Arizona Geological Society Digest, v. 14, p. 113–35.

Doelling, H. H., and Davis, F. D., 1989, The geology of Kane County, Utah, geology, mineral resources, geologic hazards: Utah Geological and Mineralogical Survey Bulletin 124, 194p.

Dover, R. J. 1969, Paleoecology of the lowermost part of the Jurassic Carmel Formation, San Rafael Swell, Emery County, Utah: Unpublished master's thesis, Utah State University, Logan, 73p.

Dunham, R. J., 1962, Classification of carbonate rocks according to depositional texture: In Ham, W. E. (ed.), Classification of carbonate rocks, a symposium: American Association of Petroleum Geologists Memoir 1, p. 108–21.

———, 1972, Guide for study and discussion for individual interpretation of the sedimentation and diagenesis of the Permian Capi-

tan geologic reef and associated rocks, New Mexico and Texas: Society of Economic Paleontologists and Mineralogists, Permian Basin Section, Publication 72–14, 235p.

Embry, A. F., Klovan, J. E., 1971, A Late Devonian reef tract on northeastern Banks Island, Northwest Territories: Canadian Petroleum Geology Bulletin, v. 19, p. 730–81.

Enos, P., 1983, Shelf environment: In Scholle, P. A., Bebout, D. G., and Moore, C. H. (eds.), Carbonate depositional environments: American Association of Petroleum Geologists Memoir 33, p. 267–95.

Folk, R. L., and Pittman, J. S., 1971, Length-slow chalcedony: A new testament for vanished evaporites: Journal of Sedimentary Petrology, v. 41, p. 1045–58.

Frakes, L. A., 1979, Climates throughout geologic time: Elsevier Scientific Publishing Co., New York, 310p.

Freeman, W. E., 1976, Regional stratigraphy and depositional environments of the Glen Canyon Group and Carmel Formation (San Rafael Group): In Hill, J. G. (ed.), Geology of the Cordilleran hinge line: Rocky Mountain Association of Geologists, p. 247–59.

Frey, R. W., 1975, The realm of ichnology—its strengths and limitations: In Frey, R. W. (ed.), The study of trace fossils: Springer-Verlag, New York, p. 13–38.

Frey, R. W., and Pemberton, S. G., 1984, Trace fossil facies models: In Walker, G. R. (ed.), Facies models (2d ed.): Geoscience Canada Reprint Series 1, p. 189–207.

Friedman, G. M., 1959, Identification of carbonate minerals by staining methods: Journal of Sedimentary Petrology, v. 29, p. 87–97.

Friedman, G. M., and Sanders, J. E., 1978, Principles of sedimentology: John Wiley and Sons, New York, 792p.

Fritz, T. R., 1977, The depositional environments of the Jurassic Carmel Formation of northeastern Utah: Unpublished master's thesis, Fort Hays State University, Kansas, 100p.

Geesaman, R. C., 1979, Sedimentary facies of the Carmel Formation, southeast Utah: Unpublished master's thesis, Northern Arizona University, Flagstaff, 150p.

Geesaman, R. C., and Voorhees, B. J., 1980, Facies and depositional tectonics of Middle Jurassic Carmel Formation, southern Utah: American Association of Petroleum Geologists Bulletin, Abstracts with Programs, v. 64, p. 712.

Gilluly, J., and Reeside, J. B., Jr., 1928, Sedimentary rocks of the San Rafael Swell and some adjacent areas in eastern Utah: U.S. Geological Survey Professional Paper 150-D, p. 61–110.

Ginsburg, R. N., 1975, Tidal deposits—a casebook of recent examples and fossil counterparts: Springer-Verlag, New York, 428p.

Goddard, E. N., Trask, P. D., De Ford, R. K., Rove, O. N., Singewald, J. T., Jr., and Overbeck, R. M., 1984, Rock-color chart: Geological Society of America, Boulder, 11p.

Gregory, H. E., 1950, Geology and geography of the Zion Park region, Utah and Arizona: U.S. Geological Survey Professional Paper 220, 200p.

Gregory, H. E., and Moore, R. C., 1931, The Kaiparowits region, a geographic and geologic reconnaissance of parts of Utah and Arizona: U.S. Geological Survey Professional Paper 164, 161p.

Gregory, H. E., and Noble, L. F., 1923, Notes on a geological traverse from Mohave, California, to the mouth of the San Juan River, Utah: American Journal of Science, v. 5, p. 229–38.

Hagan, G. M., and Logan, B. W., 1975, Prograding tidal-flat sequences—Hutchinson Embayment, Shark Bay, Western Australia: In Ginsburg, R. N. (ed.), Tidal deposits—a casebook of recent examples and fossil counterparts: Springer-Verlag, New York, p. 215–32.

Hallam, A., 1975, Jurassic environments: Cambridge University Press, New York, 269p.

Halley, R. B., Harris, P. M., and Hine, A. C., 1983, Bank margin environment: In Scholle, P. A., Bebout, D. G., and Moore, C. H. (eds.), Carbonate depositional environments: American Association of Petroleum Geologists Memoir 33, p. 463–506.

Hardie, L. A., 1977, Sedimentation on the modern carbonate tidal flats of northwest Andros Island, Bahamas: Johns Hopkins University Studies in Geology, no. 22, 202p.

Harris, P. M., 1983, The Joulters ooid shoal, Great Bahama Bank: In Peryt T. (ed.), Coated grains: Springer-Verlag, New York, p. 132–41.

Heckel, P. H., 1972, Recognition of ancient shallow-marine environments: In Rigby, J. K., and Hamblin, W. K. (eds.), Recognition of ancient sedimentary environments: Society of Economic Paleontologists and Mineralogists, Special Publication 16, p. 226–87.

Heller, P. L., Bowdler, S. S., Chambers, H. P., Coogan, J. C., Hagen, E. S., Shuster, M. W., Winslow, N. S., and Lawton, T. F., 1986, Time of initial thrusting in the Sevier orogenic belt, Idaho, Wyoming, and Utah: Geology, v. 14, p. 388–91.

Hine, A. C., 1977, Lily Bank, Bahamas; history of an active oolite sand shoal: Journal of Sedimentary Petrology, v. 47, p. 1554–81.

———, 1983, Relict sand bodies and bedforms of the northern Bahamas: Evidence of extensive early Holocene sand transport: In Peryt, T. (ed.), Coated grains: Springer-Verlag, New York, p. 116–31.

Hine, A. C., Wilber, R. J., and Neumann, A. C., 1981, Carbonate sand bodies along contrasting shallow-bank margins facing open seaways—northern Bahamas: American Association of Petroleum Geologists Bulletin, v. 65, p. 261–90.

Hinman, E. E., 1957, Jurassic Carmel–Twin Creek facies of northern Utah: Compass, v. 34, p. 102–19.

Hintze, L. F., 1986, Stratigraphy and structure of the Beaver Dam Mountains, southwestern Utah: Utah Geological Association, Publication 15, p. 1–36.

———, 1988, Geologic history of Utah: Brigham Young University Geology Studies, Special Publication 7, 202p.

Hintze, L. F., Embree, G. F., and Anderson, R. E., in press, Geologic map of the Gunlock and Motoqua Quadrangles, Washington County, Utah: United States Geological Survey Miscellaneous Field Studies, Map MF.

Illing, L. V., 1954, Bahamian calcareous sands: American Association of Petroleum Geologists Bulletin, v. 38, p. 1–95.

Illing, L. V., Wells, J. A., and Taylor, J. C. M., 1965, Penecontemporaneous dolomite in the Persian Gulf: In Pray, L. C., and Murray, R. C. (eds.), Dolomitization and limestone diagenesis—a symposium: Society of Economic Paleontologists and Mineralogists Special Publication 13, p. 89–111.

Imlay, R. W., 1953, Characteristics of the Jurassic Twin Creek Limestone in Idaho, Wyoming, and Utah: Guide to the Geology of northern Utah and southeastern Idaho: Intermountain Association of Petroleum Geologists Fourth Annual Field Conference, p. 54–62.

———, 1956, Paleogeographic maps of the United States during the Jurassic Period: In McKee E. D., Oriel, S. S., Swanson, V. E., MacLachlan, M. E., MacLachlan, J. C., Ketner, K. B., Goldsmith, J. W., Bell, R. Y., Jameson, D. J., and Imlay, R. W. (eds.), Paleotectonic maps of the Jurassic System: U.S. Geological Survey Miscellaneous Geologic Investigations, Map I-175.

———, 1957, Paleoecology of Jurassic seas in the Western interior of the United States: Geological Society of America Memoir 67, p. 469–504.

———, 1964, Marine Jurassic pelecypods from central and southern Utah: U.S. Geological Survey Professional Paper 483-C, 42p.

———, 1967, Twin Creek Limestone (Jurassic) in the western interior of the United States: U.S. Geological Survey Professional Paper 540, 105p.

———, 1980, Jurassic paleobiogeography of the conterminous United States and its continental setting: U.S. Geological Survey Professional Paper 1062, 134p.

Inden, R. F., and Moore, C. H., 1983, Beach environment: In Scholle, P. A., Bebout, D. G., and Moore, C. H. (eds.), Carbonate depositional environments: American Association of Petroleum Geologists Memoir 33, p. 211–65.

Ingamells, C. O., 1964, Rapid chemical analysis of silicate rocks: Talanta, v. 11, p. 665–66.

Ingram, R. L., 1953, Fissility of mudrocks: Geological Society of America Bulletin, v. 64, p. 869–78.

James, N. P., 1984, Shallowing-upward sequences in carbonates: In Walker, R. G. (ed.), Facies models (2nd ed.): Geoscience Canada Reprint Series 1, p. 213–28.

Keroher, G. C., 1970, Lexicon of geologic names of the United States for 1961–1967: U.S. Geological Survey Bulletin, v. 1350, 848p.

Kocurek, G., and Dott, R. H., Jr., 1983, Jurassic paleogeography and paleoclimate of the central and southern Rocky Mountains region: In Reynolds, M. W., and Dolly E. D. (eds.), Mesozoic paleogeography of west central United States: Society of Economic Paleontologists and Mineralogists, Rocky Mountain Section, p. 101–16.

Leith, C. K., and Harder, T. C., 1908, The iron ores of the Iron Springs District, southern Utah: U.S. Geological Survey Bulletin 338, 102p.

Lewis, D. W., 1986, Practical sedimentology: Hutchinson Ross Publishing Co., Stroudsburg, Pennsylvania, 229p.

Logan, B. W., 1961, Cryptozoan and associated stromatolites from the Recent, Shark Bay, Western Australia: Journal of Geology, v. 69, p. 517–33.

Logan, B. W., Davies, G. R., Read, J. F., and Cebulski, D., 1970, Carbonate sedimentation and environments, Shark Bay, Western Australia: American Association of Petroleum Geologists Memoir 13, 223p.

Logan, B. W., Rezack, R., and Ginsburg, R. N., 1964, Classification and environmental significance of algal stromatolites: Journal of Geology, v. 72, p. 68–83.

Loreau, J. P, and Purser, B. H., 1973, Distribution and ultrastructure of Holocene ooids in the Persian Gulf: In Purser, B. H. (ed.), The Persian Gulf, Holocene carbonate sedimentation and diagenesis in a shallow epicontinental sea: Springer-Verlag, New York, p. 279–328.

Lowrey, R. O., 1976, Paleoenvironment of the Carmel Formation at Sheep Creek Gap, Daggett County, Utah: Brigham Young University Geology Studies, v. 23, p. 173–203.

Lucia, F. J., 1972, Recognition of evaporite-carbonate shoreline sedimentation: In Rigby, J. K., and Hamblin, W. K. (eds.), Recognition of ancient sedimentary environments: Society of Economic Paleontologists and Mineralogists, Special Publication 16, p. 160–91.

Mackin, J. H., 1954, Geology and iron ore deposits of the Granite Mountain area, Iron County, Utah: U.S. Geological Survey Mineral Investigation Field Studies Map, MF 14.

Marvin, R. F., Wright, J. C., and Walthall, F. G., 1965, K-Ar and Rb-Sr ages of biotite from the Middle Jurassic part of the Carmel Formation, Utah: U.S. Geological Survey Professional Paper 525-B, p. 104–7.

McCarthy, W. R. 1959, Stratigraphy and structure of the Gunlock-Motoqua area, Washington County, Utah: Unpublished master's thesis, University of Washington, Seattle, 41p.

Miller, A. K., 1928, A new echinoid from the Sundance of west central Wyoming: American Journal of Science, v. 16, p. 143–46.

———, 1929, *Ancyclocidaris*, a new echinoid genus from the Sundance of west central Wyoming: American Journal of Science, v. 18, p. 334–36.

Newell, N. D., and Rigby, J. K., 1957, Geologic studies in the Great Bahama Bank: Regional aspects of carbonate deposition: Society of Economic Paleontologists and Mineralogists Special Publication 5, p. 15–79.

Nielson, D. R., 1988, Depositional environments and petrology of the Middle to Upper Jurassic Carmel Formation in the Gunlock area, Washington County, Utah: Unpublished master's thesis, Brigham Young University, Provo, Utah, 230p.

Peterson, F., 1988a, Pennsylvanian to Jurassic eolian transportation systems in the western United States: Sedimentary Geology, v. 56, p. 207–60.

———, 1988b, A synthesis of the Jurassic System in the southern Rocky Mountain region: In Geological Society of America, Decade of North American Geology, v. D-2, Sedimentary Cover—North American Craton, p. 65–76.

Peterson, F., and Pipiringos, G. N., 1979, Stratigraphic relations of the Navajo Sandstone to Middle Jurassic formations, southern Utah and northern Arizona: United States Geological Survey Professional Paper 1035-B, 43p.

Phillips, G. M., 1963, A new regular echinoid from the Jurassic of Wyoming, U.S.A.: Journal of Paleontology, v. 37, p. 1110–15.

Phoenix, D. A., 1963, Geology of the Lees Ferry area, Coconino County, Arizona: U.S. Geological Survey Bulletin 1137, 86p.

Pipiringos, G. N., and O'Sullivan, R. B., 1978, Principal unconformities in Triassic and Jurassic rocks, western interior United States—a preliminary survey: U.S. Geological Survey Professional Paper 1035-A, 29p.

Powell, J. W., 1875, Exploration of the Colorado River of the West and its tributaries: U.S. Government Printing Office, Washington, D.C., 190p.

Purser, B. H., 1973, The Persian Gulf–Holocene carbonate sedimentation and diagenesis in a shallow epicontinental sea: Springer-Verlag, New York, 471p.

Purser, B. H., and Evans, G., 1973, Regional sedimentation along the Trucial Coast, southeastern Persian Gulf: In Purser, B. H. (ed.), The Persian Gulf–Holocene carbonate sedimentation and diagenesis in a shallow epicontinental sea: Springer-Verlag, New York, p. 211–13.

Reeside, J. B., Jr., and Bassler, H., 1922, Stratigraphic sections in southwestern Utah and northwestern Arizona: U.S. Geological Survey Professional Paper 129-D, p. 53–77.

Reineck, H. E., and Singh, I. B., 1980, Depositional sedimentary environments: Springer-Verlag, New York, 549p.

Richards, H. G., 1958, Cyclic deposition in the Jurassic Carmel Formation in eastern Utah: Journal of Sedimentary Petrology, v. 28, p. 40–45.

Richter, D. K., 1983, Calcareous ooids: a synopsis: In Peryt, T. (ed.), Coated grains: Springer-Verlag, New York, p. 71–99.

Rigby, J. K., 1986a, The Carmel Formation in the Gunlock area, Beaver Dam Mountains, southwestern Utah: Utah Geological Association Publication 15, p. 55–62.

———, 1986b, Shallow-water facies in the Jurassic Carmel Formation in the Beaver Dam Mountains of southwesternmost Utah: Geological Society of America Abstracts with Programs, Rocky Mountain Section, v. 18, p. 406.

Schneider, J. F., 1975, Recent tidal deposits, Abu Dhabi, United Arab Emirates, Arabian Gulf: In Ginsburg, R. N. (ed.), Tidal deposits—a casebook of recent examples and fossil counterparts: Springer-Verlag, New York, p. 209–14.

Scholle, P. A., 1978, A color illustrated guide to carbonate rock constituents, textures, cements, and porosities: American Association of Petroleum Geologists Memoir 27, 241p.

Schultz, L. G., and Wright, J. C., 1963, Bentonite beds of unusual composition in the Carmel Formation, southwest Utah: U.S. Geological Survey Professional Paper 450-E, p. 67–72.

Scoffin, T. P., 1987, An introduction to carbonate sediments and rocks: Chapman and Hall Publishers, New York, 274p.

Shinn, E. A., 1983, Tidal flat environment: In Scholle, P. A, Bebout, D. G., and Moore, C H. (eds.), Carbonate depositional environments: American Association of Petroleum Geologists Memoir 33, p. 171–210.

Shinn, E. A., Lloyd, R. M., and Ginsburg, R. N., 1969, Anatomy of a modern carbonate tidal flat, Andros Island, Bahamas: Journal of Sedimentary Petrology, v. 39, p. 1202–28.

Siegel, F. R., 1961, Variations of Sr/Ca ratios and Mg contents in recent carbonate sediments of the northern Florida Keys area: Journal of Sedimentary Petrology, v. 31, p. 336–42.

Snoke, A. W., and Lush, A. P., 1984, Polyphase Mesozoic-Cenozoic deformation history of the northern Ruby Mountains–East Humboldt Range, Nevada: Western geological excursions: Geologic Society of America Annual Meeting Guidebook, Reno, Nevada, Mackay School of Mines, v. 4, p. 232–60.

Sohl, N. F., 1965, Marine Jurassic gastropods, central and southern Utah: U.S. Geological Survey Professional Paper 503-D, 29p.

Stanley, K. O., Jordan, W. M., and Dott, R. H., Jr., 1979, New hypothesis of Early Jurassic paleogeography and sediment dispersal for western United States: American Association of Petroleum Geologists Bulletin, v. 55, p. 10–19.

Stokes, W. L., 1952, Lower Cretaceous in Colorado Plateau: American Association of Petroleum Geologists Bulletin, v. 36, p. 951–92.

Taylor, D. W., 1981, Carbonate petrology and depositional environments of the limestone member of the Carmel Formation, near Carmel Junction, Kane County, Utah: Brigham Young University Geology Studies, v. 28, p. 117–33.

Thompson, A. E., and Stokes, W. L., 1970, Stratigraphy of the San Rafael Group, southwest and south central Utah: Utah Geological and Mineral Survey Bulletin 87, 53p. (Replacement copy issued May 1971.)

Thompson, R. W., 1968, Tidal flat sedimentation on the Colorado River delta, northwestern Gulf of California: Geologic Society of America Memoir 107, 133p.

Trask, P. D., 1937, Relation of salinity to calcium carbonate content in marine sediments: U.S. Geological Survey Professional Paper 186, 27p.

Vail, P. R., Mitchum, R. M., and Thompson, S., 1977, Seismic stratigraphy—applications to hydrocarbon exploration: In Payton, C. E. (ed.), American Association of Petroleum Geologists Memoir 26, p. 83–97.

Voorhees, B. J., 1978, Stratigraphy and facies of the lower Carmel Formation (Middle Jurassic), southwestern Utah: Unpublished master's thesis, Northern Arizona University, Flagstaff, 161p.

Walker, T. R., 1967, Formation of red beds in modern and ancient deposits: Geological Society of America Bulletin, v. 78, p. 353–68.

Wells, J. W., 1942, A new species of coral from the Jurassic of Wyoming: American Museum Novitates no. 1161, p. 1–3.

Wiley, M. S., 1963, Stratigraphy and structure of the Jackson Mountain–Tobin Wash area, southwest Utah: Unpublished master's thesis, University of Texas, Austin, 103p.

Williams, N. C., 1952, Jurassic stratigraphy of southwestern Utah: Guidebook to the geology of Utah—Cedar City, Utah, to Las Vegas, Nevada, no. 7, p. 62–77.

Wilmarth, M. G., 1938, Lexicon of geologic names of the United States: U.S. Geological Survey Bulletin 896, 1244p.

Wilson, J. L., 1975, Carbonate facies in geologic history: Springer-Verlag, New York, 471p.

Wilson, J. L., and Jordan, C., 1983, Middle shelf environment: In Scholle, P. A., Bebout, D. G., and Moore, C. H. (eds.), Carbonate depositional environments: American Association of Petroleum Geologists Memoir 33, p. 297–343.

Wright, J. C., and Dickey D. D., 1963a, Block diagram of the San Rafael Group and underlying strata in Utah and part of Colorado: U.S. Geologic Survey Oil and Gas Investigation Chart OC–63.

————, 1963b, Relations of the Navajo and Carmel Formations in southwest Utah and adjoining Arizona: In Short papers in geology, hydrology, and topography: U.S. Geological Survey Professional Paper 450-E, p. 63–67.

————, 1978a, North–south cross section of the Jurassic San Rafael Group in Utah and western Colorado: U.S. Geological Survey Open-File Report 78-965.

————, 1978b, Miscellaneous cross sections of the Jurassic San Rafael Group in southern Utah: U.S. Geological Survey Open-File Report 78–966.

Wright, J. C., and Snyder, R. P., 1979, Stratigraphic sections of Jurassic San Rafael Group and adjacent rocks in Iron and Washington Counties, Utah: U.S. Geological Survey Open-File Report 79–71318, 53p.